

Sap flow and leaf gas exchange response to drought and heatwave in urban green spaces in a Nordic city

Joyson Ahongshangbam^{1,4}, Liisa Kulmala^{2,3}, Jesse Soininen¹, Yasmin Frühauf¹, Esko Karvinen², Yann Salmon^{1,3}, Anna Lintunen^{1,3}, Anni Karvonen¹, and Leena Järvi^{1,4}

¹Institute for Atmospheric and Earth System Research (INAR)/Physics, Faculty of Science, University of Helsinki, Helsinki, Finland

²Finnish Meteorological Institute, Helsinki, Finland

³Institute for Atmospheric and Earth System Research/Forest Sciences, Viikki Plant Science Centre (ViPS), Faculty of Agriculture and Forestry, University of Helsinki, Helsinki, Finland

⁴Helsinki Institute of Sustainability Science, University of Helsinki, Finland

Correspondence: Joyson Ahongshangbam (joyson.ahongshangbam@helsinki.fi)

Abstract. Urban vegetation plays a role in offsetting urban CO₂ emissions, mitigating heat through tree transpiration and shading, and acting as deposition surfaces for pollutants. The frequent occurrence of heatwaves and concurrent drought conditions significantly disrupt the processes of urban trees, particularly their photosynthesis and transpiration rates. Despite the pivotal role of urban tree functioning in delivering essential ecosystem services, the precise nature of their response remains uncertain.

5 We conducted sap flux density (J_s) and leaf gas exchange measurements of four tree species (*Tilia cordata*, *Tilia × europaea*, *Betula pendula*, *Malus spp.*) located in different urban green areas (Park, Street, Forest, Orchard) in Helsinki, Finland. Measurements were made over two contrasting summers 2020 and 2021. Summer 2021 had a local heatwave and drought, while summer 2020 was more typical for Helsinki. In this study, we aimed to understand the responses of urban tree transpiration (measured with sap flux density) and leaf gas exchange to heatwave and drought, and examine the main environmental drivers
10 controlling the tree transpiration rate during these periods. We observed varying responses of J_s during the heatwave period at the four urban sites. When comparing the heatwave and non-heatwave periods, a 35-67% increase in J_s was observed at the Park, Forest, and Orchard locations, while no significant change was seen at the Street site. Our results also showed that J_s was higher (31-63%) at all sites during drought compared to non-dry periods. The higher J_s during the heatwave and dry periods were mainly driven by the high atmospheric demand for evapotranspiration represented by the high vapor pressure
15 deficit (VPD), suggesting that the trees were not experiencing severe enough heat or drought stress that stomatal control would have decreased transpiration. Accordingly, photosynthetic potential (A_{max}), stomatal conductance (g_s), and transpiration (E) at the leaf level did not change during heatwave and drought periods, excluding the Park site where significant reduction in g_s was seen. VPD explained 55-69% of the variation in the daily mean J_s during heatwave and drought periods at all sites. At the Forest site, the increase of J_s saturated after a certain VPD level likely due to low soil water availability during these hot and
20 dry periods. Overall, the heat and drought conditions were untypical for the region but not excessive enough to restrict stomatal control and transpiration, indicating that ecosystem services such as cooling were not at risk.

Keywords: extreme weather, drought, sap flux, transpiration, urban trees

1 Introduction

Ongoing urbanization transforms the natural environment, land cover, and ecological functions. Urbanization enhances CO₂ emissions and the urban heat island (UHI) effect, leading to harsher conditions in cities and a decrease in thermal comfort when compared to more natural surroundings (Oke et al., 1989; Roth et al., 1989). Urban green spaces have a role in offsetting anthropogenic CO₂ emissions and alleviating UHI effect, given their potential for carbon sequestration and storage, and water regulation to cool their surroundings (Lindén et al., 2016; Bowler et al., 2010; Havu et al., 2022; Hardiman et al., 2017). Several studies have highlighted the CO₂ sequestration potential of urban vegetation (Nowak and Crane, 2002; Davies et al., 2011; Muñoz-Vallés et al., 2013; Nowak et al., 2013), and addressed urban green areas as a way of mitigating GHG emissions in cities (Dhakal, 2010; Paloheimo and Salmi, 2013; Pataki et al., 2021). The role of urban trees in mitigating UHI is also well-reported in many urban studies (Rahman et al., 2019; Pataki et al., 2011). Particularly, under extremely high temperatures, the potential of urban trees in heat mitigation has been shown to be significant (Gillner et al., 2015; Schwaab et al., 2021). Trees provide cooling through two main mechanisms. Firstly, urban trees reduce surface temperature by shading, resulting in less absorption and storage of incoming short-wave radiation by surfaces. Secondly, trees cool the environment through transpiration when water taken up by roots is released through leaf stomata. The energy consumed to evaporate water from leaf stomata provides a cooling effect on the leaf surface and lowers nearby air temperature by advection. Urban trees also provide other ecosystem services such as pollutant deposition, aesthetics, recreation, soil conservation, and buffer for noise and wind (Brack, 2002; Jo, 2002; Jim and Chen, 2009; Pataki et al., 2009).

In urban conditions, trees are subjected to harsh environmental conditions, such as elevated air temperature, lower air humidity, limited soil water and nutrient availability, compared with surrounding areas (Nielsen et al., 2007). Extreme weather such as heatwaves and drought affect the physiology of urban trees and thus also their potential to mitigate the effect of extreme weather and to adapt to climate change. Hence, it is important to understand the response of the physiological processes regulating urban trees' functioning during extreme weather events.

The rise in temperature during summer heatwaves has effects on tree function both directly with increasing leaf temperature potentially leading to leaf damages (Kunert et al., 2022; Atkin and Tjoelker, 2003; Ghannoum and Way, 2011), and indirectly by increasing the vapor-pressure deficit (VPD) with consequences for transpiration and photosynthesis through stomatal control (Lloyd and Farquhar, 2008). Tree responses to heatwaves in urban areas have rarely been studied, but trees in natural forests can adapt to rising temperatures by enhancing growth and utilising water more efficiently if provided with enough moisture in the soil (Winbourne et al., 2020). However, such acclimation may not be possible for trees in urban settings as shown by their often higher foliar temperatures, which may limit photosynthesis and transpiration (Bussotti et al., 2014). Droughts have been occurring more frequently in recent times causing severe symptoms for trees even in areas that are usually considered to be rather moist such as high latitude areas (Hartmann et al., 2022). A tree usually responds to drought either by avoiding a significant decrease in water potential and relative water content through stomatal closure at the cost of reduced photosynthesis, i.e. the isohydric strategy, or by maintaining photosynthesis by keeping the stomata open at the cost of letting the water potential decrease, i.e. the anisohydric strategy (Villar-Salvador et al., 2004; De Micco and Aronne, 2012). Moreover, summer

droughts are usually associated with high air temperature further severely reducing carbon assimilation, and transpiration through lowered stomatal conductance and increasing potential leaf damages (Bussotti et al., 2014; Winbourne et al., 2020).

60 However, the specific effects of an urban environment on the trees' response to stresses such as drought and heat are not yet fully known. A few studies have investigated the potential cooling effect of urban trees during heatwaves and droughts (Gillner et al., 2015), and their impact on urban tree functions (Rötzer et al., 2021) where the urban tree functions depend on the species type, growing conditions, local climate and water availability. Nonetheless, because of the complex urban stressors and the spatial heterogeneity of urban landscapes, further studies are needed to quantify the impact of extreme events on urban trees' function. This information is especially needed for high-latitude cities because global warming is more prominent at
65 high latitudes making their urban ecosystems particularly vulnerable.

In this study, we measured a set of typical processes regulating the functions of urban trees, specifically transpiration and leaf gas exchange, during local heatwave and drought in the boreal urban environment of Helsinki, Finland. We used sap flow as a proxy for whole tree transpiration and studied its response to hot and dry periods in different urban green areas. From these measurements, we further quantified how much the different environmental factors control the sap flow rate. We addressed the
70 following research questions:

1. How does local heatwave affect the transpiration and leaf gas exchange rates of boreal urban trees?
2. How does drought affect boreal urban tree transpiration and leaf gas exchange rates?
3. What are the main environmental drivers affecting transpiration rates during local heatwave and drought in high latitude urban green areas?

75 We hypothesize that: H1) While increasing VPD during heatwaves increases the driving force for transpiration and thus sap flow, it also triggers stomatal closure, ultimately leading to a decrease in photosynthetic rates and a decoupling of VPD and leaf gas exchange rates. H2) A drought event decreases both sap flux density and the rate of photosynthesis. To answer the questions and test the hypotheses, we conducted continuous sap flux and manual leaf-gas exchange measurements at four diverse urban green areas in Helsinki during the summers of 2020 and 2021.

80 **2 Methods**

2.1 Sites description

The study was conducted near the University of Helsinki Kumpula campus, located 4 km northeast of the Helsinki city center. The Kumpula area is characterized by heterogeneous land-use cover (Figure 1a), particularly by contrasting urban vegetation. Within the study area, four sites were selected to be studied: a park with sparse trees ('Park'), a single line of roadside trees
85 ('Street'), an urban forest ('Forest'), and an apple orchard ('Orchard'). These sites are located close to a micrometeorological eddy covariance station (FI-Kmp, 60°12'11.3"N 24°57'40.4" E), which is also an Associated Ecosystem Station of ICOS (Integrated Carbon Observation System) and part of the SMEAR (Station for Measuring Ecosystem Atmosphere Relations) III station (Vesala et al., 2008; Järvi et al., 2009). Overall, Helsinki is a humid continental region (according to Köppen climate

classification), with annual precipitation of 652 mm yr^{-1} and yearly mean temperature of $6.5 \text{ }^\circ\text{C}$ during the 30-year climatic
90 reference period 1991-2020 (FMI, 2021). The summer of 2021 experienced elevated temperatures at $21.6 \text{ }^\circ\text{C}$, which were 21%
higher, along with minimal rainfall at 86 mm, showing a 51% deficit compared to the reference period.

The urban park (Park; Figure 1b) is located in the Kumpula botanical garden, southwest of the FI-Kmp measurement tower.
The study site is characterized by *Tilia cordata* trees and a ground layer of short vegetation comprised mainly of lawn species,
clovers (*Trifolium repens*) and mosses. The ground vegetation was mowed daily using an automatic mowing device, leaving
95 the clippings on-site and irrigation was activated on dry and warm days within the wider park area. The daily mowing and
irrigation were restricted in the area around the studied trees (0.25 ha area) during the measurement period but the tree roots
reached the irrigated area.

The roadside plantation (Street; Figure 1c) is located on the road called Hermannin rantatie, 0.8 km east of the FI-Kmp
measurement tower. It consists of a row of *Tilia × europaea*, a hybrid of *T. cordata* and *T. platyphyllos*. It is the most commonly
100 planted urban tree in Helsinki and Nordic countries in general, comprising 44% of Helsinki's Street trees (Sjöman et al., 2012).
The street trees grow over a patch of soil spreading 60 m long and 2.7 m wide, with an average tree spacing of 8.2 m. Normally,
the trees are regularly trimmed and maintained by the city gardening company, but they were non-managed during our study.

The urban forest (Forest; Figure 1d) is a small forest patch ($25 \times 30 \text{ m}^2$) located between the FI-Kmp measurement tower
in the north and the Kumpula botanical garden in the south. This site is dominated by mature *Betula pendula* trees, but other
105 deciduous trees such as *Betula pubescens*, *Alnus glutinosa*, *Acer platanoids*, and *Ulmus glabra* are also growing at the site. The
sparse ground vegetation layer consists mainly of *Aegopodium podagraria* and bare spots. This site was the only non-managed
study site and was regenerated naturally.

The apple orchard (Orchard; Figure 1e) is located in the Kumpula school garden 0.9 km west of the FI-Kmp measurement
tower. The site is characterized by scattered apple trees (20 trees per $30 \text{ m} \times 30 \text{ m}$ area) planted over a managed lawn. There
110 was no irrigation. The lawn in our measurement area was manually mown a few times during the summers.

More detailed descriptions of all four sites are given in Table 1 and soil properties, particularly soil water retention prop-
erties, are presented in Appendix A1. All sites were equipped with continuous measurements of sap flux and meteorological
variables from June 2020 to September 2021, except the Orchard site, where data were recorded only from June to Septem-
ber 2021. Manual leaf gas exchange measurements accompanied the continuous measurements during the summer months
115 (June-August).

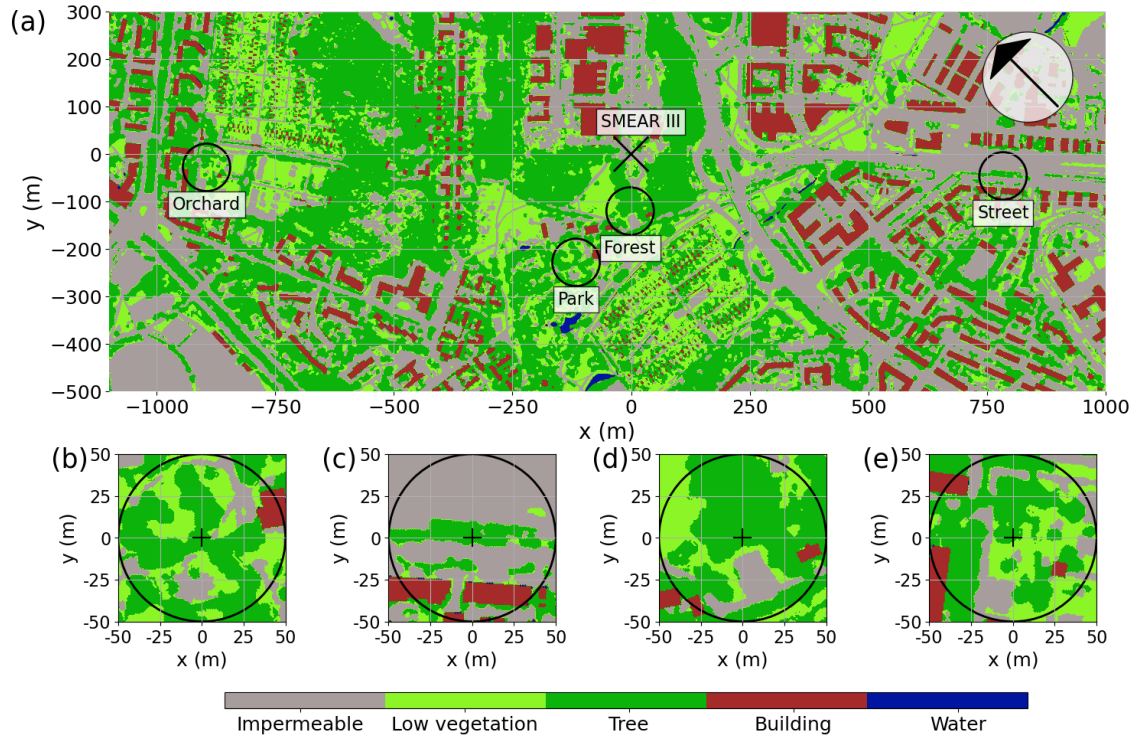


Figure 1. (a) Surface cover of the study area in Helsinki (StromJan, 2020) with the location of the FI-Kmp station at SMEAR III and the monitoring sites as well as the local surface covers at the (b) Park, (c) Street, (d) Forest, and (e) Orchard measurement sites.

Table 1. The four study sites with information on their location, the dominating tree species, the mean diameter at breast height (DBH), sapwood area, and height of the selected three individuals, years since plantation (age), and soil particle type.

	Park	Street	Forest	Orchard
Latitude	60°12'08.4"N	60°11'51.6"N	60°12'07.7"N	60°12'30.17"N
Longitude	24°57'21.4"E	24°58'13.2"E	24°57'33.0"E	24°56'57.77"E
Tree species	<i>Tilia cordata</i>	<i>Tilia × europaea</i>	<i>Betula pendula</i>	<i>Malus spp.</i>
Drought strategies	Mildly Isohydic ¹	Isohydic ²	Isohydic ³	Isohydic ⁴
DBH (cm)	26.3	19.5	23.6	30
Sapwood area (cm²)	433.8	271.9	349.7	397.0
Height (m)	12.5	10	22	6.5
Age (years)	26	34	35	72 (approx.)
Soil type	Sand moraine	Fine sand moraine	Sand moraine	Sand clay

¹Leuschner et al. (2019) ²Liu et al. (2022); Kunert and Tomaskova (2020) ³Zapater et al. (2013) ⁴Lauri et al. (2011)

2.2 Sap flux measurements

Sap flux measurements were conducted using the Thermal Dissipation Probe (TDP; Granier, 1985). TDP sensors consist of needles (20-30 mm long) equipped with thermocouples, where the downstream needle acts as a heating probe and the upstream needle as a reference probe. The thermocouples measure the temperature difference between the heated probe and the reference probe, which is used to calculate the sap flux density. Sap flux density can be scaled up to estimate the whole-tree water use. In our study, we selected three trees at each site (for a total of 12 trees) based on high sun exposure and dominant position. In each tree, a TDP sensor was inserted into the stem xylem at a height of 1.3 m. A vertical distance of 10 cm was kept between the heated and the reference probe. In the Street and Forest sites, the sensors were installed at 2 m height to avoid damage or disturbance from pedestrians. The sensors were installed on the northern side of the stem. The installed sensors were insulated with reflective aluminum foil to protect them and minimize the thermal gradient's effect. The temperature difference (dT) was recorded every 1 min using a datalogger (Datataker DT80M). The sap flux density (J_s , $\text{g cm}^{-2}\text{h}^{-1}$) was calculated at 1 min interval based on Graniers' equation (eqn 1):

$$J_s = 42.84 * ((dT_{max} - dT)/dT)^{1.231}, \quad (1)$$

where dT_{max} is the maximum dT where zero J_s was observed. Zero flux condition was based on Lu et al. (2004), which was derived as the average local daily maximum dT of seven consecutive nights. Processing of raw sap flux data was conducted in R (RStudio Team, 2020). Further, daily tree water use was calculated by multiplying the daily sap flux density with the sapwood area. For *Tilia cordata*, *Tilia × europaea* and *Betula pendula*, the sapwood area was derived from the literature using species-specific allometric equations based on trunk diameter (Gebauer et al., 2008; Hernandez-Santana et al., 2015) and for Orchard, we calculated the sapwood area by coring the stem of the apple trees. For further analysis, the sap flux density data were selected only for the growing season (June to September) for 2020 and 2021. Only sunny days data were considered to compare the sap flux density of the four sites. Sunny days were selected based on the following criteria: the daily total R_g was greater than 200 W m^{-2} , there was no precipitation, and the mean daytime vapor pressure deficit (VPD) was greater than 0.33 kPa (Riikonen et al., 2016). Sap flux data were averaged to half-hourly, daily, and monthly values for each measured tree. In addition, we normalized the sap flux density using VPD by dividing the half-hourly J_s by the corresponding half-hourly VPD data. This was done to remove the effect of VPD and also to examine the dependency of J_s on other environmental variables during these heatwave and drought periods.

2.3 Leaf gas exchange

Leaf gas exchange rates were measured using a portable gas exchange system (Walz GFS-3000, Heinz Walz, GmbH, Germany) with a standard measuring head (8 cm^2 cuvette, $2 \times 4 \text{ cm}$). At each site, measurements were done during the summers of 2020 and 2021 at approximately four-week intervals from the trees equipped with TDP sensors. However, at the Park site, one different tree was selected for leaf gas exchange measurements to replace one of the sap flow-equipped trees as it was difficult to reach its canopy with a man lift. The measurements were recorded on the southern or southwestern side of the trees and

conducted mainly during local morning time (8 AM-12 PM). At the Park site, measurements were made at three canopy heights (top, middle, and bottom), whereas at the Street and Forest sites, only two heights (the top and bottom) were monitored. At the Orchard site, only one measurement was made in the middle of the canopy of each tree. The measurements were performed on one healthy leaf per tree and canopy height.

During each measurement, the CO₂ level was set to 415 ppm. The temperature was left to and follow the ambient conditions. To screen out any potentially damaged leaves, a different leaf was selected from the same branch if the assimilation rate during the first 10 min of the measurement was very low (under 1.5 μmol m⁻² s⁻¹). The measurement steps involved setting photosynthetically active radiation (PAR) at 1200 μmol m⁻² s⁻¹ for 12 minutes and then increasing to a level of 1500 μmol m⁻² s⁻¹. After reaching the maximum level, PAR was gradually decreased down to <1 μmol m⁻² s⁻¹ over 43 minutes. Altogether, 15 different PAR intensities were included. A simple light response curve was fitted to the net CO₂ exchange ($NE(PAR)$, μmol m⁻² s⁻¹), as follows:

$$NE(PAR) = (A_{max} * PAR) / (\hat{I}^2 + PAR) - R, \quad (2)$$

where R is the leaf respiration i.e., NE measured at PAR = 0 (μmol m⁻² s⁻¹), A_{max} (μmol m⁻² s⁻¹) is the maximum rate of photosynthesis and β (μmol m⁻² s⁻¹) is the half-saturation constant describing the light intensity where photosynthesis rate is half of A_{max} .

From the above fitting, only A_{max} is considered in our analysis. Other variables of leaf gas exchange, namely stomatal conductance (g_s , mmol m⁻² s⁻¹) and transpiration (E , mmol m⁻² s⁻¹) were also recorded during the measurements. Maximum stomatal conductance and transpiration were calculated based on momentary g_s and E at PAR = 1100 μmol m⁻² s⁻¹.

During the manual measurement campaigns in the summer of 2021, three leaf samples per site were also monthly collected in order to measure their relative water content (RWC). The samples were collected during the late afternoon (4 PM) and the fresh weight (FW) was measured. After that, the leaf samples were soaked overnight and turgid weight (TW) was measured. Later on, the samples were oven-dried at 60 Â°C for 24h, and the dry weight (DW) was measured. The RWC was calculated based on the equation below:

$$RWC(\%) = ((FW - DW) / (TW - DW)) * 100, \quad (3)$$

2.4 Meteorological and soil data

At all four sites, meteorological variables, including air temperature (Air T, °C) and relative humidity (RH, %) were measured at a height of 1.5-1.8 m with a weather sensor (HMP110, Vaisala, Vantaa, Finland, at Park, Street and Forest sites; HC2A, Rotronic, Bassersdorf, Germany, at Orchard site). Soil sensors (Hydra-probe 2 SDI-12, Stevens, Oregon, USA, except ML3 ThetaProbe, Delta-T, Cambridge, UK, sensors in the Orchard) were installed at 10 and 30 cm depth to measure soil temperature (Soil T, °C) and soil moisture (SM, m³ m⁻³). Data were recorded continuously at 1-minute intervals and then converted into half-hourly averaged data. Furthermore, the vapor pressure deficit (VPD, kPa) was calculated using Air T and RH based on saturated vapor pressure. Photosynthetically active radiation (PAR, W m⁻²) and precipitation data were collected from the

180 SMEAR III station FI-Kmp measurement tower and roof of a nearby building, respectively (Vesala et al., 2008; Järvi et al., 2009).

2.5 Detection of local heatwave and drought period

According to Fischer and Schär (2010), a heatwave is defined as a spell of at least six consecutive days with maximum temperatures exceeding the local 90th percentile of the control period. Accordingly, in our study, heatwave (Appendix A1) was defined against a control period spanning from 1991 to 2020. Further, our study period was categorized into four periods: 185 heatwave (17 June 2021 to 18 July 2021), pre-heatwave (1 June 2021 to 16 June 2021), post-heatwave (19 July 2021 to 31 August 2021) and no heatwave (1 July 2020 to 31 July 2020) periods with mean daily maximum air temperatures of 26.4 °C, 21.5 °C, 20.4 °C and 19.6 °C, respectively. The daily maximum air temperature during the heat period ranged from 20.5 to 30.2 °C, with a mean daily difference of 6 °C (ranging from 1.8 to 10.8 °C) above the average temperature in the control 190 period.

To determine the drought period, a monthly Standardised Precipitation-Evapotranspiration Index (SPEI, (Vicente-Serrano et al., 2010) was calculated, indicating that June (SPEI = -1.4) and July 2021 (SPEI = -0.8) had moderate drought conditions. Here, we considered days with precipitation less than 1 mm and mean relative extractable soil water (REW) at the depth of 10 cm less than 0.45 as a dry period for all sites. As a result, the dry period was from 22 June 2021 to 27 July 2021 and 195 wet period from 28 July 2021 to 31 August 2021. We calculated the REW from the soil moisture data, field capacity and wilting point of the site according to Granier et al. (1999), where the wilting point and field capacity of sandy loam (Park, Street and Forest) are 10 % and 22.9 %, respectively and those of clay (Orchard) are 25 % and 38.4 %, respectively, based on Hagemann and Stacke (2015).

Taking into account the partial overlap between the heatwave and dry periods, we also identified three stress periods: only 200 heat (17 June 2021 - 22 June 2021), both heat-dry (23 June 2021 - 18 July 2021) and only dry (19 July 2021 - 27 July 2021).

2.6 Statistical analysis

To test the hypotheses, Kruskal Wallis test followed by Dunn's posthoc test was performed to examine differences in J_s and leaf gas exchange variables (A_{max} , g_s and E) between the different climatic periods (dry/wet/heatwave/post-heatwave/no heatwave). First, polynomial regression with 2nd order degree was fitted between daytime mean J_s and daytime mean VPD. 205 Second, multiple linear regression analysis was performed to determine the effect of the meteorological variables on J_s . The tested variables were VPD, PAR, soil moisture, and soil temperature at 30 cm. The relative importance of each meteorological variable in controlling the daily J_s was assessed using the t statistic from the multiple linear regression summary. Data processing (post-processing of sap flux, meteorological and gas exchange data) statistical analysis and visualization were conducted in Python (Python version 3).

3.1 Weather conditions

The summer of 2021 (particularly July) was warm and dry, as compared to the summer of 2020, and the climatic reference period (1991–2020). The mean air temperature in July 2021 was 21.6 °C, being 21% higher than that in July 2020 (16.7 °C) and 19% higher than the average July temperature during the climatic reference period (18.1 °C) (Figure 2a). At the four urban
 215 sites, high air temperature (20.2–21.6 °C), high soil temperature (15.7–18.5 °C), high VPD (0.9–1.1 kPa), and low soil moisture (0.1–0.4 m³ m⁻³) were observed during July 2021 (Figure 3 for the Park site, Figures A2, A3 and A4 for the other sites). The total precipitation for June and July 2021 (86 mm) was 51% lower than for June and July 2020 (177 mm) and 27% lower than precipitation on average for the climatic reference period (117 mm) (Figure 2b).

The climatic conditions differed between the four sites during the summer of 2021. The mean of the meteorological variables
 220 (air temperature, VPD, soil temperature, and soil moisture) during the summer months (June, July, and August) 2021 were considered for comparison. Higher mean air temperature was observed at both Orchard (19.2 °C) and Street sites (19.3 °C) as compared to Forest (17.9 °C) and Park (17.8 °C) sites (Table 2). Similar mean VPD was found at the Orchard (0.78 kPa), Park (0.75 kPa), and Forest sites (0.75 kPa), but VPD was 11% higher at the Street site (0.84 kPa). Also, the mean soil temperature at the Street site (19.9 °C) was 24–34% higher than at the Park (16.1 °C), Orchard (15.2 °C) and Forest sites (14.8 °C).
 225 The soil water availability varied from 13% to 25% (Figure A1). Mean soil moisture differed between sites, the Orchard site having the highest values (0.37 m³ m⁻³), and the Forest site the lowest (0.09 m³ m⁻³) while the Park and Street sites had intermediate values at 0.13 and 0.22 m³ m⁻³, respectively. Soil moisture increased after rainfall events at all the sites except the Forest site, where soil moisture remained low throughout the late summer after the hot and dry July 2021 (Figure A3).
 The climatic conditions differed between the four sites during the summer of 2021. The mean of the meteorological variables
 230 (air temperature, VPD, soil temperature, and soil moisture) during the summer months (June, July, and August) 2021 were considered for comparison. Higher mean air temperature was observed at both Orchard (19.2 °C) and Street sites (19.3 °C) as compared to Forest (17.9 °C) and Park (17.8 °C) sites (Table 2). Similar mean VPD was found at the Orchard (0.78 kPa), Park (0.75 kPa), and Forest sites (0.75 kPa), but VPD was 11% higher at the Street site (0.84 kPa). Also, the mean soil temperature at the Street site (19.9 °C) was 24–34% higher than at the Park (16.1 °C), Orchard (15.2 °C) and Forest sites (14.8 °C). The soil
 235 water availability varied from 12.9% to 25% (Table A1). Mean soil moisture differed between sites as the Orchard site having the highest values (0.37 m³ m⁻³), and the Forest site the lowest (0.09 m³ m⁻³) while the Park and Street sites had intermediate values at 0.13 and 0.22 m³ m⁻³, respectively. Soil moisture increased after rainfall events at all the sites except the Forest site, where soil moisture remained low throughout the late summer after the hot and dry July 2021 (Figure A3).

3.2 Variability in sap flow rate in 2021

240 On sunny days, the mean daily water use of the trees in the Park, Street, Forest and Orchard were 0.32 ± 0.01 kg cm⁻² day⁻¹, 0.42 ± 0.01 kg cm⁻² day⁻¹, 0.20 ± 0.01 kg cm⁻² day⁻¹ and 0.46 ± 0.01 kg cm⁻² day⁻¹, respectively (Figure 4a), differing significantly from each other (P<0.05). The mean daytime sap flux density (J_s) for the summer period (June-August) was the

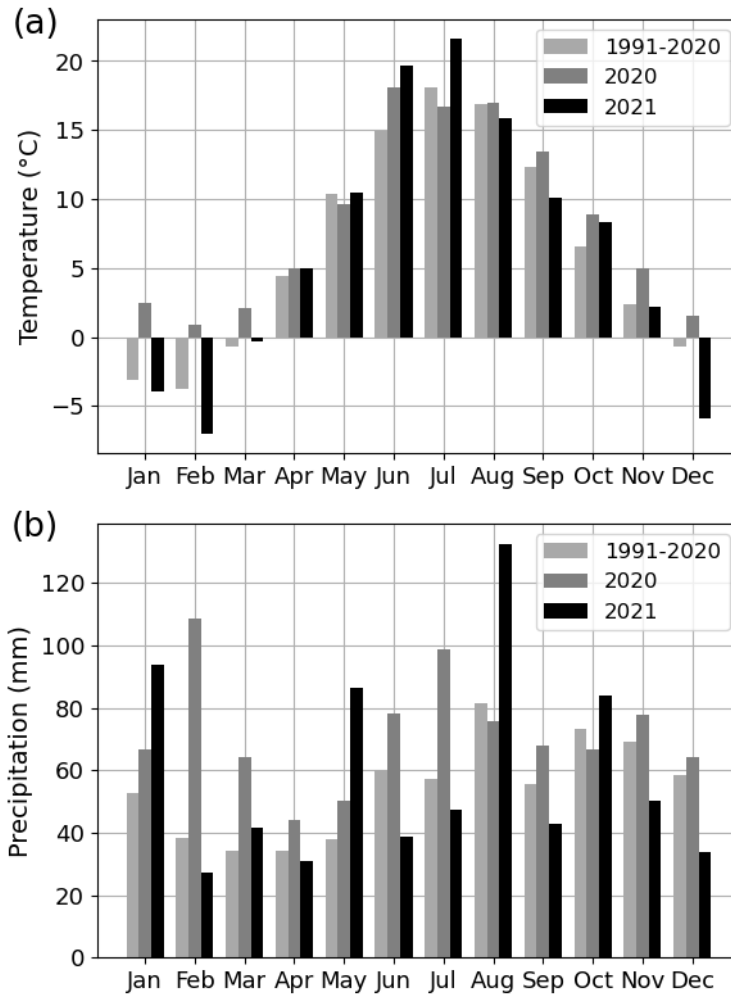


Figure 2. (a) Monthly mean air temperature and (b) monthly total precipitation for the years 2020 and 2021, and the climatic reference period of 30 years (1991-2020).

highest at the Orchard site with $20.6 \pm 0.3 \text{ g cm}^{-2} \text{ h}^{-1}$, the lowest with $8.1 \pm 0.1 \text{ g cm}^{-2} \text{ h}^{-1}$ at the Forest site, and $14.4 \pm 0.2 \text{ g cm}^{-2} \text{ h}^{-1}$ and $17.7 \pm 0.3 \text{ g cm}^{-2} \text{ h}^{-1}$ at the Park and Street sites, respectively. The monthly mean J_s differed significantly especially between July and September at the four sites ($P < 0.05$) (Figure 4b).

3.3 The effect of heatwave on sap flux density

During the heatwave period, the mean sap flow rates of the trees at the Park, Street, Forest and Orchard sites were $0.38 \pm 0.02 \text{ kg cm}^{-2} \text{ day}^{-1}$, $0.42 \pm 0.02 \text{ kg cm}^{-2} \text{ day}^{-1}$, $0.24 \pm 0.01 \text{ kg cm}^{-2} \text{ day}^{-1}$ and $0.52 \pm 0.02 \text{ kg cm}^{-2} \text{ day}^{-1}$, respectively. At the Park site, the mean J_s during the heatwave period was 59% higher than during the no heatwave period and 39% higher than

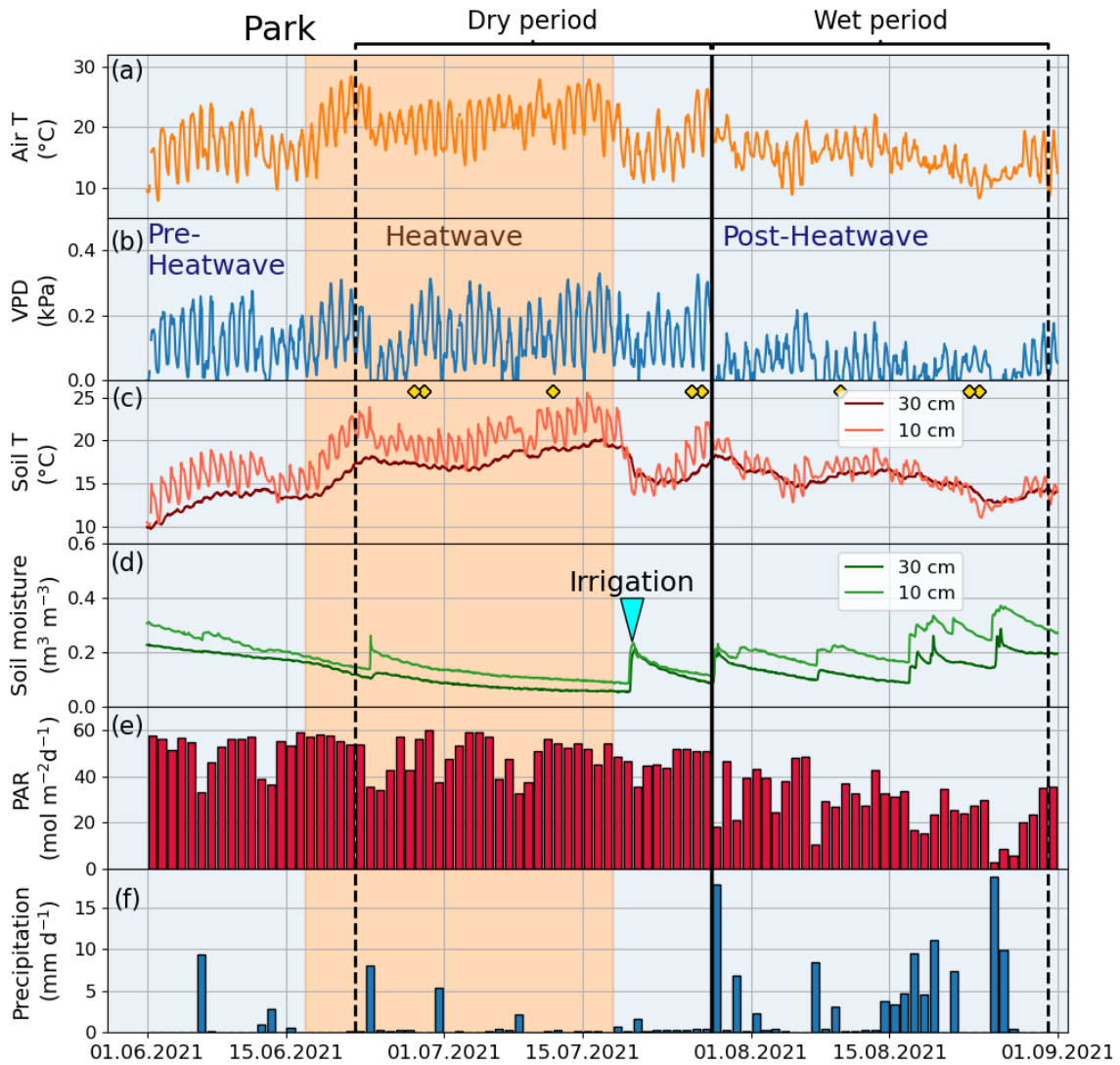


Figure 3. Meteorological and soil data from 2021 showing hourly a) air temperature (Air T), b) water vapor deficit (VPD), c) soil temperature (Soil T) and d) soil moisture measured at the Park site, and e) daily mean Photosynthetically active radiation (PAR) and daily sum precipitation data measured at the SMEARIII station. The orange shading indicates the heatwave period during the summer of 2021 and the black vertical line indicates the onset of the wet period. The yellow markers in panel (c) denote the manual leaf gas measurement dates.

250 during the post-heatwave period but there was no significant difference with the pre-heatwave period. At the Street site, there was no significant difference in the mean J_s between the heatwave, no heatwave, pre-heatwave and post-heatwave periods. At the Forest site, the mean J_s during the heatwave period was 13% higher than during the pre-heatwave and 67% higher than during the post-heatwave periods. At the Orchard site, the mean J_s during the heatwave period was 35% higher than during the

Table 2. Monthly mean air temperature (Air T, °C), mean vapor pressure deficit (VPD, kPa), mean soil temperature (Soil T, °C) and mean soil moisture content ($\text{m}^3 \text{m}^{-3}$) for the four study sites in 2021.

		Air T	VPD	Soil T	Soil moisture
Park	June	18.4	0.84	14.4	0.16
	July	20.2	0.96	17.5	0.09
	August	14.8	0.45	14.7	0.15
	September	8.7	0.40	11.0	0.19
Street	June	19.8	0.93	18.5	0.23
	July	21.6	1.07	22.8	0.25
	August	16.1	0.51	18.5	0.25
	September	10.0	0.40	12.7	0.29
Forest	June	18.0	0.77	13.1	0.16
	July	20.7	1.01	16.9	0.07
	August	15.2	0.48	14.5	0.06
	September	8.7	0.34	11.2	0.06
Orchard	June	21.1	0.81	15.5	0.44
	July	21.1	1.05	15.7	0.28
	August	15.7	0.49	14.6	0.40
	September	9.4	0.35	12.9	0.49

post-heatwave period but there was no significant difference with the pre-heatwave period (Figure 5a, $P < 0.05$). At the Forest and Orchard sites, no data were recorded during the no heatwave period.

When normalized with VPD, there were no significant differences in J_s between the heatwave, no heatwave, pre-heatwave and post-heatwave periods in the Park, Forest or Orchard (Figure 5b). At the Street site, normalized J_s during the heatwave period was 33% lower than during the no heatwave period and 7% lower than during the pre-heatwave period, but no difference were observed with the post-heatwave period.

260 3.4 The effect of drought on sap flux density

During the dry period, the mean sap flow rates at the Park, Street, Forest and Orchard sites were $0.36 \pm 0.02 \text{ kg cm}^{-2} \text{ day}^{-1}$, $0.42 \pm 0.01 \text{ kg cm}^{-2} \text{ day}^{-1}$, $0.20 \pm 0.01 \text{ kg cm}^{-2} \text{ day}^{-1}$ and $0.50 \pm 0.02 \text{ kg cm}^{-2} \text{ day}^{-1}$, respectively. Mean J_s was significantly higher during the dry period than during the wet period at all sites (Figure 6a, $P < 0.05$). At the Park, Street, Forest and Orchard sites, mean J_s were 66%, 31%, 43% and 53% higher during dry period than wet period, respectively.

265 Normalized J_s was significantly lower during dry than wet period at all sites, with a reduction of 16%, 48%, 28% and 26% in normalized J_s during the dry period at the Park, Street, Forest and Orchard sites, respectively (Figure 6b).

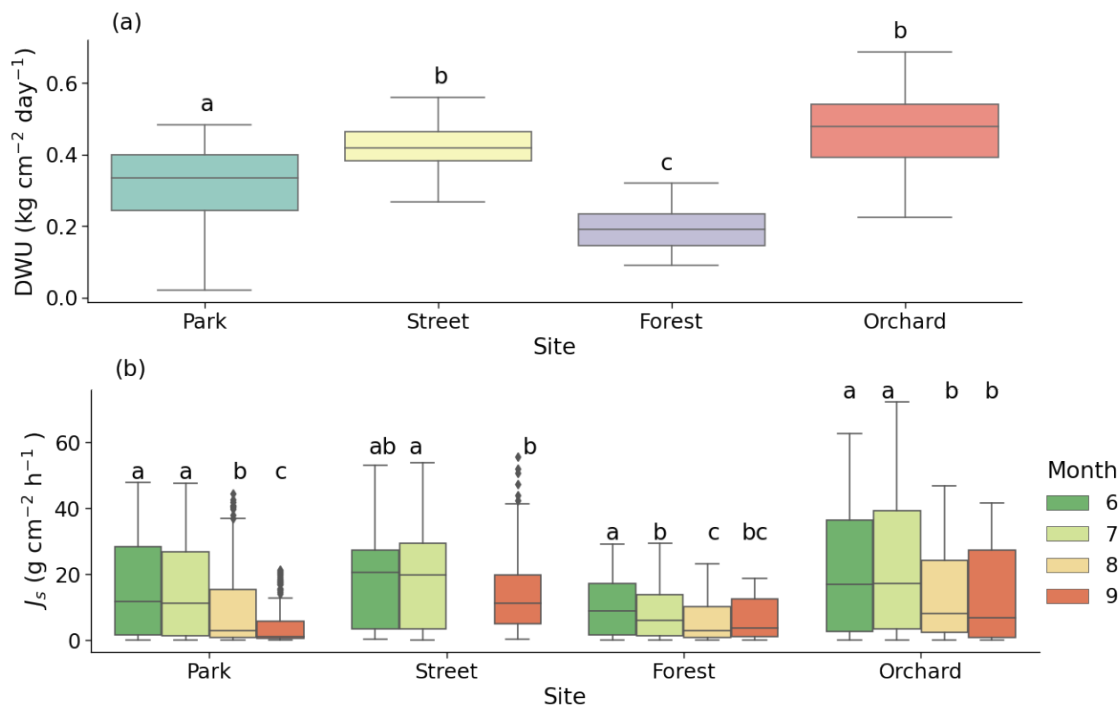


Figure 4. (a) Daily water use (DWU) of the trees and (b) monthly mean sap flux density (J_s) at the four urban vegetation sites: Park (*Tilia cordata*), Street (*Tilia × europaea*), Forest (*Betula pendula*) and Orchard (*Malus spp.*). The letters indicate the significant differences between the (a) sites and (b) monthly mean J_s at each site ($P < 0.05$). Note: data was non-available for August at the Street site due to technical problems.

Considering the partial overlap of the heatwave and dry period, we identified three stress periods: only heat (17 June 2021 - 22 June 2021), both heat-dry (23 June 2021 - 18 July 2021) and only dry (19 July 2021 - 27 July 2021) and analysed the effect of only heat, only dry and both heat-dry on sap flux density. This analysis revealed that the effect of heat was relatively stronger than the effect of drought or both heat and drought at the Park, Forest and Orchard sites, while at the Street site, the effect of heat, drought and both were similar (Figure A6).

3.5 Leaf gas exchange during the heatwave and drought periods

We compared leaf gas exchange variables, namely A_{max} , g_s and E , between the different heatwave periods and between dry and wet periods (Table 3). No significant differences in these three variables were found at the Park, Forest and Orchard sites between the different heatwave periods; however, at the Street site, A_{max} and E were significantly ($P < 0.05$) higher during heatwave than post-heatwave periods but there was no significant difference as compared to the no heatwave period. Also, g_s showed no difference between the different heatwave periods at the Street site.

Table 3. Averages of leaf gas exchange variables: Maximum assimilation (A_{max} , $\hat{\mu}\text{Emol m}^{-2} \text{s}^{-1}$), Stomatal Conductance (g_s , $\text{mmol m}^{-2} \text{s}^{-1}$), and Transpiration (E, $\text{mmol m}^{-2} \text{s}^{-1}$) during heatwave, no heatwave, pre-heatwave and post-heatwave periods and during dry and wet periods at the four sites. The letters indicate significant differences between the various heatwave periods or drought periods. No data were available at the Street site during pre-heatwave and at the Orchard site during no heatwave period.

Site	Type / Period	A_{max}	g_s	E
Park	heatwave	13.6 $\hat{\mu}\pm$ 1.3	112.1 $\hat{\mu}\pm$ 14.1	1.5 $\hat{\mu}\pm$ 0.1
	pre-heatwave	13.6 $\hat{\mu}\pm$ 1.3	123.5 $\hat{\mu}\pm$ 0	1.9 $\hat{\mu}\pm$ 0
	post-heatwave	15.3 $\hat{\mu}\pm$ 1.1	141.3 $\hat{\mu}\pm$ 11	1.1 $\hat{\mu}\pm$ 0.1
	no heatwave	17.2 $\hat{\mu}\pm$ 1.4	147.8 $\hat{\mu}\pm$ 15.5	1.5 $\hat{\mu}\pm$ 0.1
	dry	15.0 $\hat{\mu}\pm$ 0.8	114.5 $\hat{\mu}\pm$ 7.7 ^a	1.5 $\hat{\mu}\pm$ 0.1
	wet	14.3 $\hat{\mu}\pm$ 2.0	163.3 $\hat{\mu}\pm$ 17.5 ^b	1.7 $\hat{\mu}\pm$ 0.2
Street	heatwave	10.9 $\hat{\mu}\pm$ 1.0 ^a	91.4 $\hat{\mu}\pm$ 7.3	1.2 $\hat{\mu}\pm$ 0.1 ^a
	pre-heatwave	-	-	-
	post-heatwave	6.6 $\hat{\mu}\pm$ 0.8 ^b	64.2 $\hat{\mu}\pm$ 12.0	0.8 $\hat{\mu}\pm$ 0.1 ^b
	no heatwave	8.7 $\hat{\mu}\pm$ 1.2 ^a	73.0 $\hat{\mu}\pm$ 11.1	0.8 $\hat{\mu}\pm$ 0.1 ^a
	dry	10.9 $\hat{\mu}\pm$ 1.0 ^a	91.4 $\hat{\mu}\pm$ 7.3	1.2 $\hat{\mu}\pm$ 0.1
	wet	6.6 $\hat{\mu}\pm$ 0.8 ^b	64.2 $\hat{\mu}\pm$ 12.0	0.8 $\hat{\mu}\pm$ 0.1
Forest	heatwave	16.4 $\hat{\mu}\pm$ 1.0	105.7 $\hat{\mu}\pm$ 17.8	1.3 $\hat{\mu}\pm$ 0.2
	pre-heatwave	16.3 $\hat{\mu}\pm$ 0	128.4 $\hat{\mu}\pm$ 0	1.5 $\hat{\mu}\pm$ 0
	post-heatwave	10.7 $\hat{\mu}\pm$ 2.9	104.2 $\hat{\mu}\pm$ 31.2	1.1 $\hat{\mu}\pm$ 0.3
	no heatwave	17.4 $\hat{\mu}\pm$ 2.3	133.5 $\hat{\mu}\pm$ 12.1	1.4 $\hat{\mu}\pm$ 0.1
	dry	16.4 $\hat{\mu}\pm$ 1.0	105.7 $\hat{\mu}\pm$ 17.8	1.3 $\hat{\mu}\pm$ 0.2
	wet	10.7 $\hat{\mu}\pm$ 2.9	104.2 $\hat{\mu}\pm$ 31.2	1.1 $\hat{\mu}\pm$ 0.3
Orchard	heatwave	14.1 $\hat{\mu}\pm$ 0.7	126.8 $\hat{\mu}\pm$ 5.4	0.7 $\hat{\mu}\pm$ 0.2
	pre-heatwave	13.3 $\hat{\mu}\pm$ 0	125.3 $\hat{\mu}\pm$ 0	2.0 $\hat{\mu}\pm$ 0
	post-heatwave	13.6 $\hat{\mu}\pm$ 1.0	157.3 $\hat{\mu}\pm$ 12.9	1.8 $\hat{\mu}\pm$ 0.1
	no heatwave	-	-	-
	dry	13.1 $\hat{\mu}\pm$ 1.4	135.4 $\hat{\mu}\pm$ 13.6	1.6 $\hat{\mu}\pm$ 0.1
	wet	14.0 $\hat{\mu}\pm$ 0.9	170.9 $\hat{\mu}\pm$ 20.4	1.9 $\hat{\mu}\pm$ 0.2

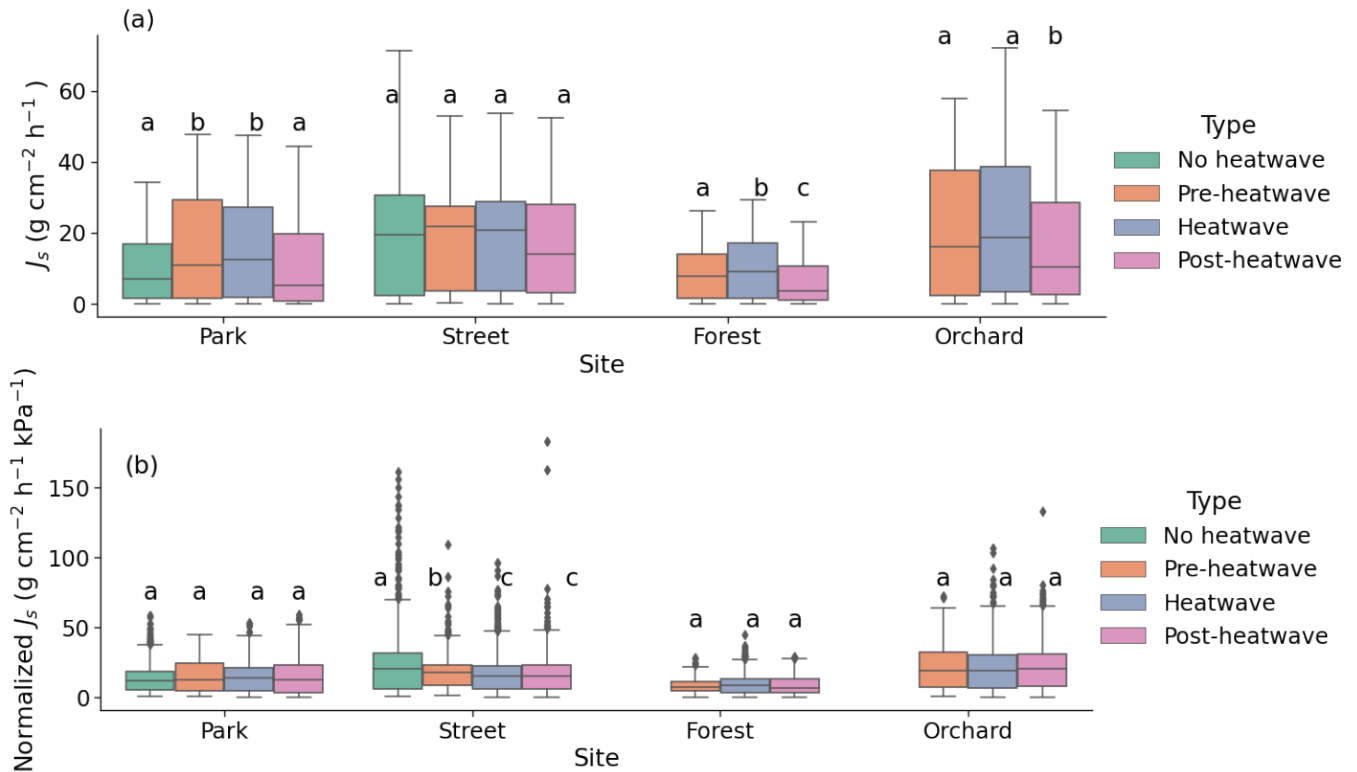


Figure 5. Sap flux densities at the four urban vegetation sites during different periods regarding a heatwave: a) mean J_s of the whole day and (b) mean normalized J_s by VPD on sunny days. The letters indicate the significant differences between the different periods within each site ($P < 0.05$).

Comparing leaf gas exchange variables between dry and wet periods, we found that at the Street site, A_{max} was significantly higher ($P < 0.05$) during dry period than wet period but no significant differences in g_s and E between dry and wet periods were found. Also, at the Park site, g_s was found to be significantly lower ($P < 0.05$) during dry period than wet period. At the Forest and Orchard sites, no significant differences were found in A_{max} , g_s and E between dry and wet periods.

The monthly relative leaf water content (RWC) as a proxy of leaf water potential was found to be lower (4-35 %) during July as compared to June and August at the Forest and Orchard sites. However, RWC was found to be higher (5-8 %) during July than the other summer months at Park and Street sites (Appendix A5).

285 3.6 Environmental control on sap flux density

We tested the relationship between the daily daytime mean VPD and J_s using 2^{nd} order polynomial regression (Figure 7, Table 4). VPD explained the variation in J_s less during the heatwave than during post-heatwave and pre-heatwave except for Forest where the VPD was not a significant driver at all during pre-heatwave. During wet period, VPD explained a higher share of the

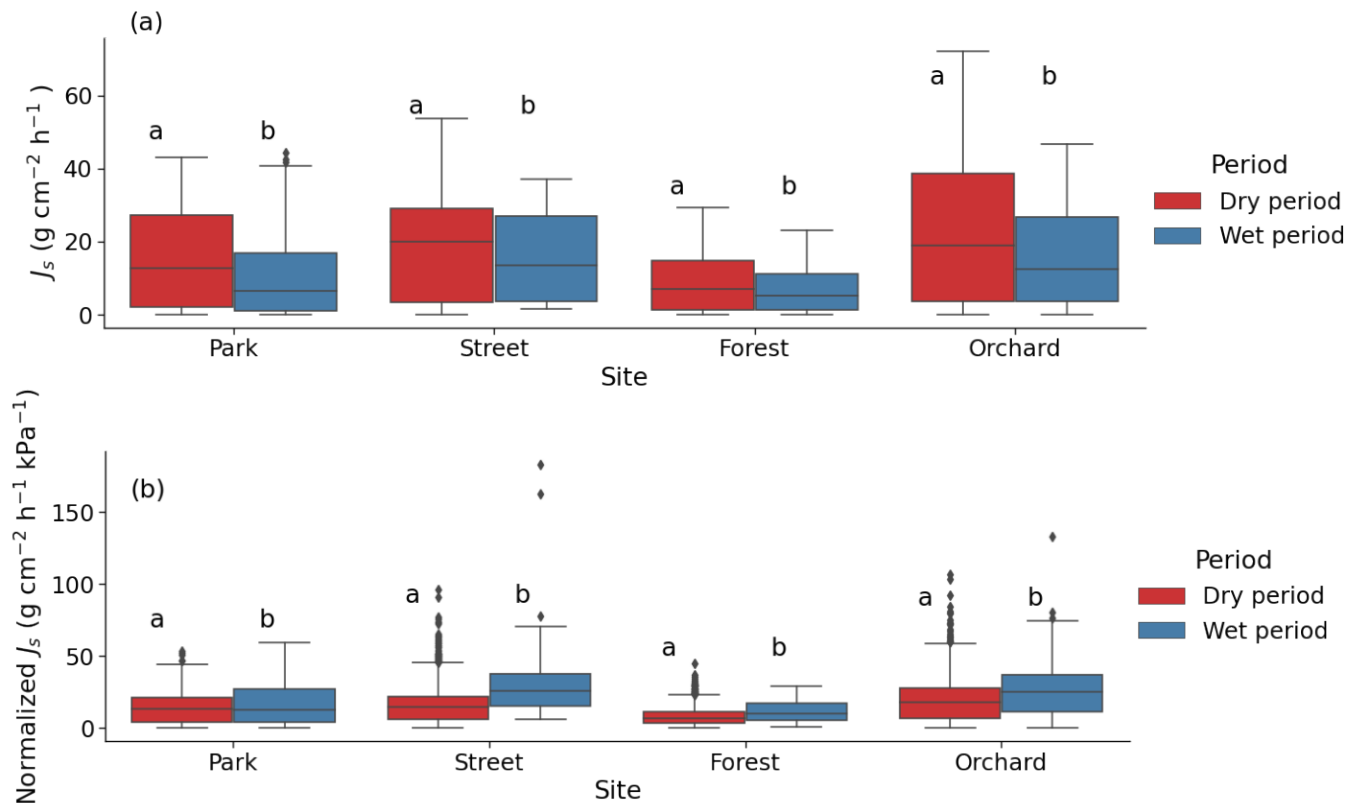


Figure 6. Sap flux density (J_s) during dry and wet periods at the four study sites. Based on sunny days, (a) data represented mean J_s of the whole day and (b) normalized J_s by VPD. The letters indicate significant differences in J_s between dry and wet periods at each site ($P < 0.05$)

variation of J_s at Park, Forest and Orchard sites. At Street site, the data availability was low and thus, the relationship could not be tested during wet period (Figure 7).

Multiple linear regression between J_s and a number of environmental variables (VPD, PAR, Soil T and SM) showed that PAR and VPD were the significant drivers for J_s at the Park, Street and Orchard sites but PAR was the only significant driver at the Forest site (Table 5). In addition, soil moisture was a significant variable in certain circumstances at certain sites, such as, in Park during heatwave and dry periods and in Forest during post-heatwave, dry and wet periods i.e. in the latter part of the growing season in general.

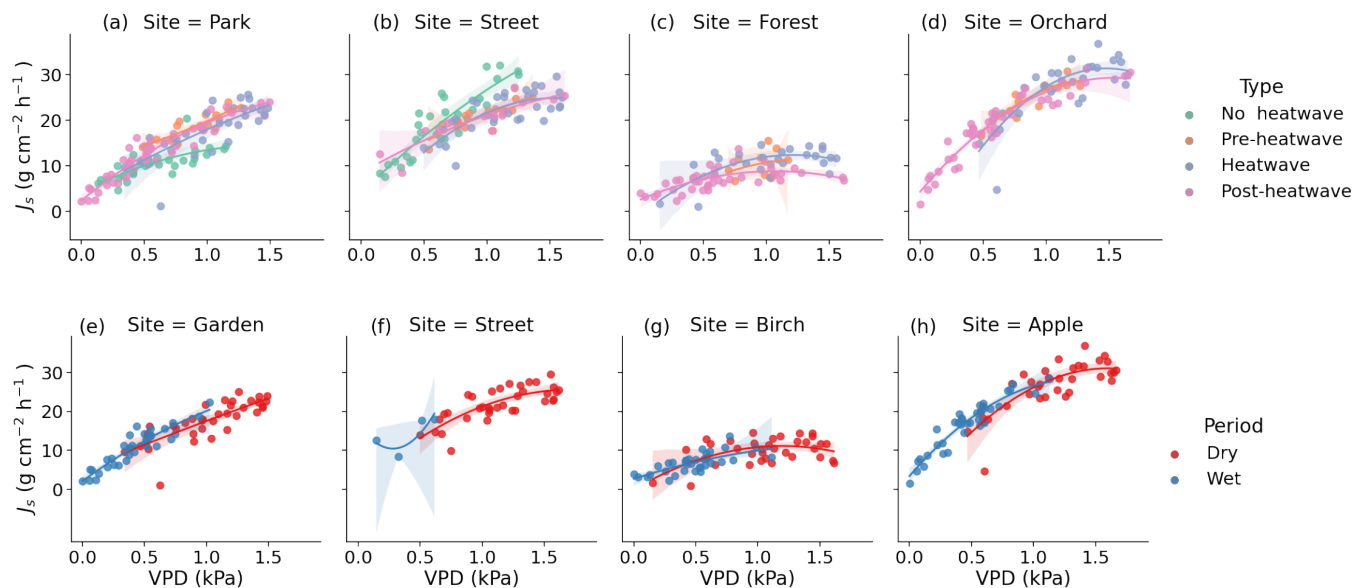


Figure 7. Observed (dots) and modeled (lines) relationship between the daytime mean daily VPD and J_s during the different heatwave periods as well as dry and wet periods. Panels (a),(b),(c), and (d) show the relationship between VPD and J_s at the Park, Street, Forest and Orchard site, respectively, during the different heatwave periods. Panels (e),(f),(g), and (h) show the relationship between VPD and J_s at the Park, Street, Forest and Orchard site, respectively, during the dry and wet periods. The model is 2nd order polynomial fit (see Table 4).

Table 4. Relationship between vapor pressure deficit and daily mean sap flux density using 2nd order polynomial fit (see Fig. 7). The values indicate the squared coefficient of correlation (adj R^2) between the two variables. Relationships statistically significant at 0.05, 0.01 and 0.001 levels are marked with *, ** and *** respectively and non-significant as ns.

	no heatwave	pre-heatwave	heatwave	post-heatwave	dry	wet
Park	0.53***	0.73***	0.57***	0.90***	0.60***	0.85***
Street	0.80***	0.62***	0.55***	0.75***	0.58***	0.22 ^{ns}
Forest	-	0.16 ^{ns}	0.43***	0.44***	0.25**	0.48***
Orchard	-	0.77***	0.69***	0.91***	0.67***	0.90***

4 Discussion

In this study, we assessed the response of urban tree water use and leaf gas exchange during hot and dry summer 2021, across four urban green areas in Helsinki. Results indicated increased sap flux density in trees during the hot and dry periods, whereas carbon assimilation, stomatal conductance, and leaf-level transpiration remained largely unaffected. Sap flux density increase in such periods varied among the studied urban sites with distinct tree species and growth conditions. VPD emerged as the primary factor influencing tree water use in the heatwave and dry conditions. In summary, the urban trees in our study

Table 5. Multiple linear regression between daily mean sap flux density and various environmental drivers (VPD, PAR, Soil temperature and Soil moisture) as independent variables. t stat value indicates the relative importance of the variables in controlling the daily sap flux variations. Relationships statistically significant at 0.05, 0.01 and 0.001 levels are marked with *, ** and *** respectively and non-significant as ns.

Site		All data	no heatwave	pre-heatwave	heatwave	post-heatwave	dry period	wet period
Park	R ²	0.63	0.59	0.75	0.74	0.93	0.74	0.92
	Intercept	5 (1.4) ^{ns}	-1.6 (-0.2) ^{ns}	-16.6 (-0.9) ^{ns}	-25.15 (-1.6) ^{ns}	4.1 (1.1) ^{ns}	-13.9(-1.1) ^{ns}	3.0 (0.7) ^{ns}
	VPD	9 (7.6)***	6.2 (3.1)***	9.1 (3.5)***	10.4 (5.1)***	9.3 (8.0)***	9.5 (5.2)***	11.0 (5.7) ^{ns}
	PAR	0.01 (3.5)***	0.01 (1.14) ^{ns}	0.01 (1.4) ^{ns}	0.03 (3.1)***	0.02 (5.4)***	0.02 (3.6)***	0.01 (4.1)**
	Soil T	-0.1 (-0.3) ^{ns}	0.5 (1.1) ^{ns}	1 (1.4) ^{ns}	0.8 (1.32) ^{ns}	-0.1 (-0.6) ^{ns}	0.4 (0.7) ^{ns}	0.03 (0.1) ^{ns}
	SM	-9.4 (-1.0) ^{ns}	-10.5 (-0.4) ^{ns}	45.6 (1.0) ^{ns}	79.6 (2.3)***	-8.0 (-1.0) ^{ns}	48.1 (2.1)***	-15.9 (-2.2) ^{ns}
Street	R ²	0.73	0.84	0.65	0.71	0.75	0.71	-
	Intercept	5.9 (2.27)*	6.2 (0.3) ^{ns}	7.0 (1.0) ^{ns}	10.6 (1.1) ^{ns}	40.7 (1.3) ^{ns}	22.5 (2.0) ^{ns}	-
	VPD	9.3 (7.8)**	17.5 (6.4)***	7.6 (2.5)*	4.6 (2.6)*	6.1 (1.4) ^{ns}	5.9 (3.4)***	-
	PAR	0.03 (7.1)**	0.02 (2.5)*	0.02 (1.7) ^{ns}	0.03 (4.4)***	0.01 (1.0) ^{ns}	0.03 (4.0)***	-
	Soil T	-0.3 (-3.3)**	-0.5 (-0.9) ^{ns}	0.07 (0.2) ^{ns}	-0.1 (-0.5) ^{ns}	-1.1 (-1.2) ^{ns}	-0.7 (-1.6) ^{ns}	-
	SM	12.6 (2.4)*	12.0 (0.2) ^{ns}	-9.7 (-0.7) ^{ns}	-13.9 (-1.0) ^{ns}	-34.5(-0.5) ^{ns}	-8.3 (-0.8) ^{ns}	-
Forest	R ²	0.56	-	0.93	0.67	0.68	0.63	0.72
	Intercept	2.4 (1.4) ^{ns}	-	91.0 (2.4) ^{ns}	-2.3 (-0.1) ^{ns}	-16.2(-1.8) ^{ns}	-17.7(-2.1)*	-17.3(-1.5) ^{ns}
	VPD	2.1 (2.0) ^{ns}	-	2.9 (1.5) ^{ns}	3.5 (1.7) ^{ns}	-0.3 (-0.3) ^{ns}	2.9(1.9) ^{ns}	0.1(0.03) ^{ns}
	PAR	0.02 (5.1)***	-	0.01 (1.3) ^{ns}	0.02 (3.4)***	0.02(4.99)***	0.02(3.6)***	0.02(3.5)***
	Soil T	-0.1 (-1.1) ^{ns}	-	-1.0 (-0.9) ^{ns}	-0.6 (-0.8) ^{ns}	-0.8 (-4.4)***	0.01(0.03) ^{ns}	-0.8(-3.4)**
	SM	-1.4 (-0.2) ^{ns}	-	-345.0 (-3.1)*	137.7 (1.1) ^{ns}	515.0(3.6)***	222.1(5.0)***	515.2(2.8)**
Orchard	R ²	0.89	-	0.86	0.77	0.93	0.74	0.92
	Intercept	9.8 (1.7) ^{ns}	-	-88.2 (-2.3) ^{ns}	57.9 (0.8) ^{ns}	27.0 (2.2)*	-31.2(-1.4) ^{ns}	3.1 (0.8) ^{ns}
	VPD	9.2 (8.0)***	-	5.9 (1.9) ^{ns}	5.4 (2.1) ^{ns}	7.8 (5.4)***	7.1 (3.4)**	11 (5.8)***
	PAR	0.04 (8.2)***	-	0.03 (2.9)*	0.05 (4.5)***	0.04 (7.6)***	0.05 (4.9)***	0.02 (4.07)***
	Soil T	-0.5 (-1.5) ^{ns}	-	0.6 (0.5) ^{ns}	-2.8 (-0.7) ^{ns}	-1.6 (-2.1)*	2.1 (1.6) ^{ns}	0.03 (0.1) ^{ns}
	SM	1.5 (0.4) ^{ns}	-	160.3 (3.2)*	-32.3 (-1.5) ^{ns}	-2.9 (-0.8) ^{ns}	-1.6 (-0.2) ^{ns}	-15.9(-2.2)***

Values indicate coefficient (*t*)^{sig}

exhibited typical functioning during the summer of 2021, suggesting that the hot and dry conditions did not induce significant physiological changes or adjustments. However, we found some interesting insights that we will discuss further in this chapter.

4.1 Site variability

305 Our study observed that the four urban vegetation sites in Helsinki exhibit variable climatic conditions where air temperature under the canopy, soil temperature, and soil moisture content were different. The highest air and soil temperatures were measured at the Street site, where impervious surfaces increase the temperatures due to heat storage. The high air temperature at the Orchard site is due to exposure of the site to direct sunlight throughout the day, heating the garden. Also, the high soil moisture at the Orchard site is mainly due to the difference in soil type, where the sand clay in the Orchard has higher water
310 holding capacity than the sand moraine soil type at the other three sites. At the Street site, VPD was higher than at the other three sites because of the higher air temperature likely due to the larger cover of impervious surfaces. Similar variability of meteorological conditions between different urban forests was found in Los Angeles metropolitan city, where the urban forests located near the city were warmer with higher VPD and lower photosynthetically active radiation as compared to the urban forests situated closer to the coast (Pataki et al., 2011). Among 10 different tree species in the city of Basel (Switzerland), the
315 tree crown temperature was lower in the park than in the street although the study reported species-specific differences in the cooling effect of urban trees (Leuzinger et al., 2010). Indeed, the difference in microclimatic conditions has been observed to vary depending on the type of vegetation, the composition of the species, the amount of green cover and the impervious surface in urban vegetation (Perini and Magliocco, 2014; Kjellgren and Clark, 1992). Also, many other studies have shown high variability in transpiration across different urban green areas (Pataki et al., 2011; McCarthy and Pataki, 2010; Sushko et al.,
320 2021). For example, in the high-latitude city of Gothenburg (Sweden), *T. europaea* had two times higher daytime transpiration rates in a park compared to a street site (Konarska et al., 2016). Although the asymmetric measurement setup in our study limits us from comparing the sites statistically we observed that Street sites had the highest sap flow rate during the summer of 2021 and the lowest at the Forest site, and we speculate that the differences might be related to growing conditions such as high soil moisture content and tree species. The sap flow rate of *Tilia cordata* at the Park was lower than that of *Malus spp* at
325 the Orchard and *Tilia × europaea* at the Street but higher than that of *Betula pendula* at the Forest site. The low sap flow rate of *Betula pendula* at the Forest site could be explained by the rather strong stomatal control typical for *Betula pendula*, i.e. it closes the stomata easily during dry conditions (Zapater et al., 2013), whereas *Tilia cordata* found at the Park site has less sensitive stomatal control (Leuschner et al., 2019), i.e. it keeps stomata open even in mild drought as it can tolerate drought better than *Betula Pendula*. Other studies in the streets of Munich and Helsinki have reported variability of transpiration rates,
330 mainly due to the differences in tree species. In Munich, the water use of *Tilia cordata Mill.* was three times higher than water use of *Robinia pseudoacacia L.* tree in the (Rahman et al., 2019) and in the street trees of Helsinki, *Alnus glutinosa* have four times higher tree water use than *Tilia × vulgaris* (Riikonen et al., 2016).

4.2 Transpiration rate and leaf gas exchange during drought and heatwave

We observed varying responses of sap flux density during heatwave and drought periods at the studied sites. At the Park, Forest, and Orchard sites, J_s increased by 35-67% during the heatwave compared to periods of no heatwave and post-heatwave, whereas the heatwave did not affect J_s in the Street site. The pre-heatwave period did not differ from the heatwave period in terms of J_s in the Park and Orchard sites, but there was a slight increase (13%) at the Forest site during the heatwave period. J_s was significantly higher during the dry period than wet period at all sites. The leaf gas exchanges such as A_{max} , g_s , and E did not change during the heatwave and dry period, thus, indicating no changes in the photosynthetic potential during these periods. Hence, we conclude that the weather was not yet severe enough to give support to our study hypotheses H1 and H2.

VPD is the driving force for transpiration, so an increase in VPD leads to an increase in J_s unless stomata in the leaves close to limit transpiration. The VPD was a significant driver for J_s during all periods and at all sites, which indicates the substantial role of VPD; however, the relative importance of VPD over daily sap flow variation differed at the four sites and during different periods of heatwave and drought. The response of sap flow to changes in VPD was less sensitive during heatwave and drought periods than during the other periods (Table 4). In theory, these results could indicate that the trees limited their water transport via stomatal control in harsh conditions. However, that was not captured by the leaf-level measurements, which on the other hand, may not represent the conditions over the different periods as well as these automatic measurements. Moreover, the leaf-level values were based on single-day measurements, which might not fully represent our study's heatwave or drought periods. Together, these results indicate that the observed increase in transpiration at the studied sites was caused by an increase in the driving force for transpiration, VPD.

Stomatal control limits plant transpiration during drought. For example, Rötzer et al. (2021) found a substantial reduction of 63% in the transpiration rate in urban *Tilia cordata* and *Robinia pseudoacacia* trees in the city of Würzburg, Germany during the European drought in 2018. During the dry period of this study, soil moisture content was notably reduced, ranging from 18% to 62% less compared to the wet period across all four locations. Similarly, during the heatwave period, the soil moisture content dropped significantly, ranging from 30% to 58% lower than the pre-heatwave period at all sites, except for the Street site. The availability of soil moisture at the Street site allowed an increase in A_{max} and E during the heatwave period. However, the observed reductions in soil moisture did not seem to be enough to cause strong stomatal regulation of transpiration (i.e., no change in g_s except for the Park site). At the Park site, the relative decrease in g_s might be due to the influence of soil moisture reduction during the dry period and also due to the isohydric behavior typical for *Tilia cordata* growing in the Park. Also, previous studies reported that transpiration during the local extreme high temperature was maintained when there was sufficient water availability in the soil in different urban green sites in Los Angeles Metropolitan, the US (Pataki et al., 2011). Similarly, previous studies have shown that VPD is a significant driver for sap flow in *Tilia × vulgaris* street trees in Helsinki (Riikonen et al., 2016), and VPD and solar radiation for daytime transpiration rates in seven different tree species, including *Betula pendula*, studied in Gothenburg, Sweden (Konarska et al., 2016). Similarly to our results regarding the Park site, Konarska et al. (2016) also found that the maximum stomatal conductance was reduced by 50% in the studied species in Gothenburg even though transpiration rate remained high during dry conditions compared to wet conditions.

During the heatwave and the dry period, VPD explained most of the variation in the daily mean J_s at the Park (57-60%), Street (55-58%) and Orchard sites (62-69%). Similarly, previous studies in high latitude cities have reported that VPD correlates well with J_s in street trees (adj. $R^2 = 0.74$) in Helsinki, Finland (Riikonen et al., 2016), and in urban trees ($R^2=0.44-0.75$) in
370 Gothenburg, Sweden (Konarska et al., 2016). Also, in Boston, Massachusetts, VPD has been shown to correlate with J_s ($R^2 = 0.63$, (Winbourne et al., 2020)). However, VPD did not explain daily variation in J_s at the forest site of our study. Also, J_s saturated after reaching certain VPD levels, especially at Forest and Orchard sites, and the saturation took place already in relatively low VPD levels in the case of the Forest site. The difference in saturation levels may be species-specific or caused by differences in soil moisture availability as the Orchard site had higher soil moisture than the Forest site during the heatwave and
375 dry period. J_s in *Tilia* at the Park and Street sites seemed to be more linearly correlated with VPD, i.e., transpiration continued to increase with increasing VPD during the stressful periods. With sufficient water supply by irrigation, less saturation with VPD was observed in urban trees previously (Winbourne et al., 2020; Marchin et al., 2022). Similarly, the non-saturation of J_s with high VPD observed at the Park site may be due to irrigation during the dry period. Several previous studies on urban trees have shown that the relationship between VPD and transpiration is species-specific and it is more typical that VPD increases
380 linearly in diffuse-porous trees but saturates in ring-porous trees (Bush et al., 2008; Rahman et al., 2019). All the species studied here are diffuse-porous.

In addition to VPD, J_s was also influenced by other environmental variables. The relative importance of soil moisture, soil temperature and solar radiation in influencing J_s differed significantly between the four studied urban sites. PAR was among the main environmental drivers of J_s at Park, Orchard and Street sites, whereas PAR alone influenced J_s at the Forest site (Table
385 5). Soil temperature was significantly related with J_s only at the Street site. When the different climatic periods were analyzed separately, soil conditions (moisture and/or temperature) affected J_s during heatwave (t stat = 2.3, $P < 0.05$) and dry periods (t stat = 2.1, $P < 0.05$) at the Park site, but not at the Street, Forest and Orchard sites. This can be explained by the irrigation provided at the Park site during the dry period. Overall, VPD and PAR were the main environmental variables influencing the urban tree transpiration during hot and dry conditions and the relative importance of these two varied depending on the tree
390 species, growing conditions and irrigation practices.

The elevated levels of transpiration (represented by high J_s) observed in the studied green areas during the heatwave indicate the presence of transpirational cooling. This phenomenon could hold substantial promise for alleviating extreme heat conditions caused by exceedingly high temperatures. Trees at the Orchard and Street sites had the highest transpiration rates, and trees in the Forest had the lowest transpiration rates during the dry and heatwave periods. These differences were mainly due to tree
395 species, their drought strategies (Gillner et al., 2017) and growing conditions of the sites, particularly soil moisture availability. Lower transpiration in *Betula pendula* at the Forest site indicates that *Betula pendula* trees growing in an urban forest do not cool the environment as much as *Tilia* or *Malus*. Several previous studies have reported that the transpirational cooling effect of urban trees during hot and dry days increases or sustains the transpiration rates to prevent excessive heat accumulation (Gillner et al., 2015; Duarte et al., 2016; Drake et al., 2018; Urban et al., 2017; Ibsen et al., 2021). Keeping the stomata
400 open in hot and dry conditions cools down the internal leaf temperatures, enabling maintaining photosynthesis (De Kauwe et al., 2019; Urban et al., 2017; Drake et al., 2018). The response depends on the species tolerance to drought, water use

efficiency, microclimatic conditions, and site heterogeneity (Bussotti et al., 2014; Winbourne et al., 2020; Rennenberg et al., 2006). Especially *Tilia cordata* is known for its mildly isohydric behavior (i.e., stomatal control is not strong) during heat and drought and an associated increase in transpiration rates causing a cooling effect in different urban conditions (Moser et al., 2017). However, also *Betula pendula*, which typically shows isohydric behavior (i.e., strong stomatal control), increased J_s during the heatwave and dry periods in the present study. Contrasting and species-specific responses of trees to heat and drought have been observed in several urban trees (Gillner et al., 2017; Osonne et al., 2014) whereas, in our study, a relatively constant responses was observed between the studied species.

Our study was limited regarding detailed comparison of tree species-specific responses or the effect of urban site type on the responses as the studied tree species were different in different site types. Also, the limited measurements of leaf gas exchange (i.e. point measurements) did not allow us to study in detail the leaf-level water during the local extreme periods. Further study capturing the effect of site conditions and tree species behavior separately would be helpful in addressing the main factors affecting the different responses of urban vegetation during heatwaves and dry periods.

5 Conclusions

We conclude that the heat and drought in Helsinki in 2021 were still not extreme enough to damage or dampen the gas exchange functioning of urban trees. Against our hypotheses, photosynthetic potential was not reduced due to lowered stomatal conductance during heatwave and drought conditions. The transpiration and photosynthetic potential during these periods remained high, suggesting stable ecosystem services such as cooling and carbon sequestration during relatively rough conditions. However, the significant role of VPD in tree water use during heatwave and drought periods was evident in our study, but its overall significance decreased during drought periods. Our finding demonstrated that meteorological definitions of weather extremes must not be necessarily directly translate into extreme biological responses and also the Nordic perspective on a heatwave is characterized by rare occurrences of air temperatures significantly lower than those seen in lower latitudes. The observed responses in tree transpiration during hot and dry periods across the four urban green areas are mainly due to VPD, and further investigations would be needed to differentiate the role of other factors such as growing conditions (soil water availability), tree species and tree size with dedicated sampling design and with the help of more complex modelling. As urbanization and the occurrence of extreme weather events are increasing, the role of urban green areas in mitigating climate change and cooling local microclimate is becoming even more significant. Further studies on the cooling potential of urban trees will provide a better understanding and support mitigation strategies and city planning in the future.

Data availability. Datasets of sap flux density, meteorological and leaf gas exchange measurements at the four urban sites in Helsinki can be found from Ahongshangbam et al. (2023).

Appendix A

Table A1. The soil properties of the four urban vegetation sites. Soil sample analyzed from the top 30 cm of soil.

	Park	Street	Forest	Orchard
Soil type	Sand moraine	Fine sand moraine	Sand moraine	Sandy clay
Bulk density (kg/l)	1.15	1.07	1.14	1.02
Main particle size distribution	66% sand 21% silt 8% clay	48% sand, 26% silt, 11% clay	71% sand 15% silt 11% clay	27% sand, 31% silt, 42% clay
Carbon content (%)	3.7	3.3	3.9	3.9
Nitrogen content (%)	0.252	0.168	0.329	0.32
C:N ratio	14.8	21.8	11.9	12.3
pH	5.6	7.2	6.5	5.9
Soil porosity	41.6 %	41.6 %	41.6 %	46.1 %
Field capacity	22.9 %	22.9 %	22.9 %	38.4 %
Wilting point	10 %	10 %	10 %	13.4 %
Available water capacity	12.9 %	12.9 %	12.9 %	25.0 %

*Available water capacity = Field capacity - Wilting point

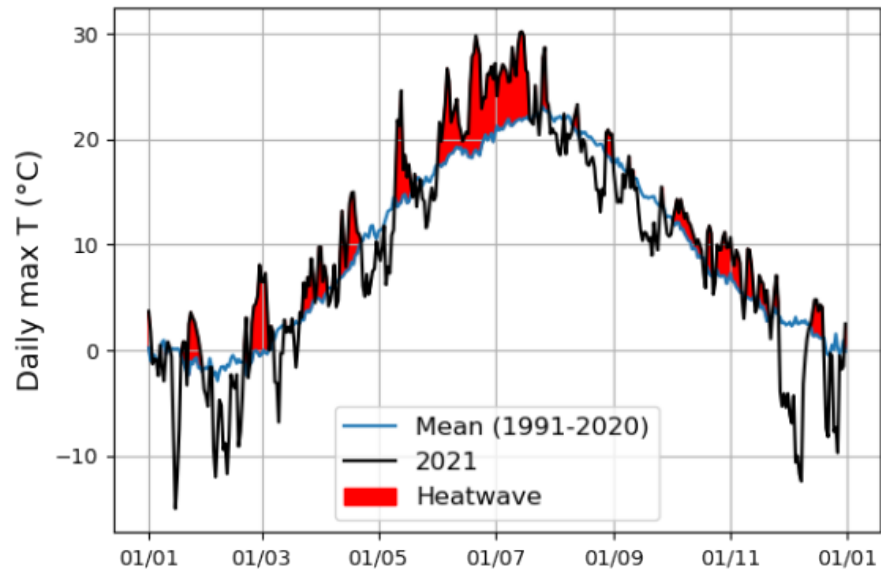


Figure A1. Heatwave detection using the daily maximum air temperature summer 2021 and the control period (1991-2020). The red color indicates the period where the daily maximum air temperature in the summer of 2021 exceeded the control period.

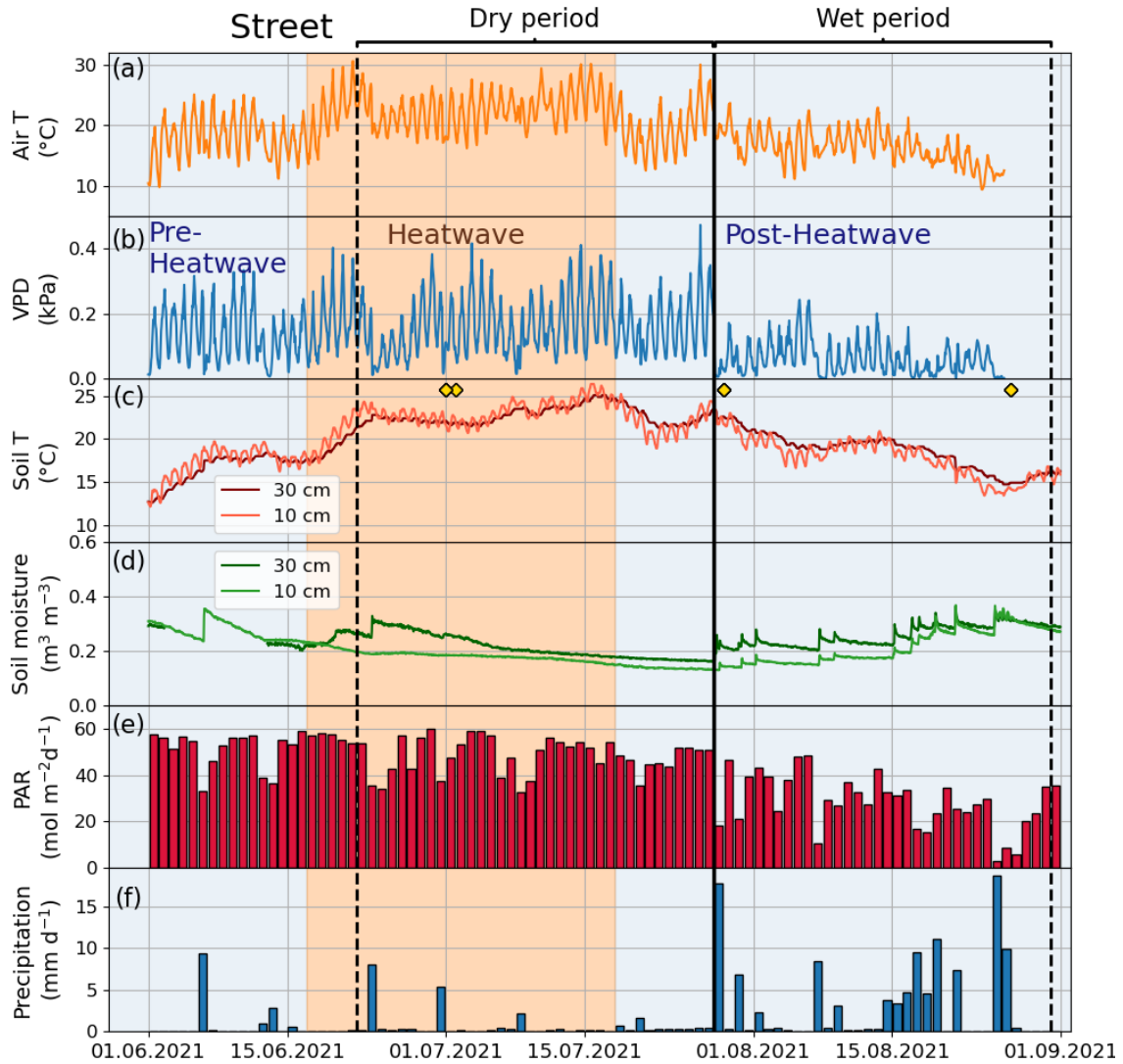


Figure A2. Meteorological condition at the Street site showing hourly a) air temperature (Air T), b) water vapor deficit (VPD), c) soil temperature (Soil T) and d) soil moisture measured and e) daily mean photosynthetically active radiation (PAR) and daily sum precipitation data measured at the SMEARIII station. The yellow markers in panel (c) denote the dates of manual leaf gas measurements.

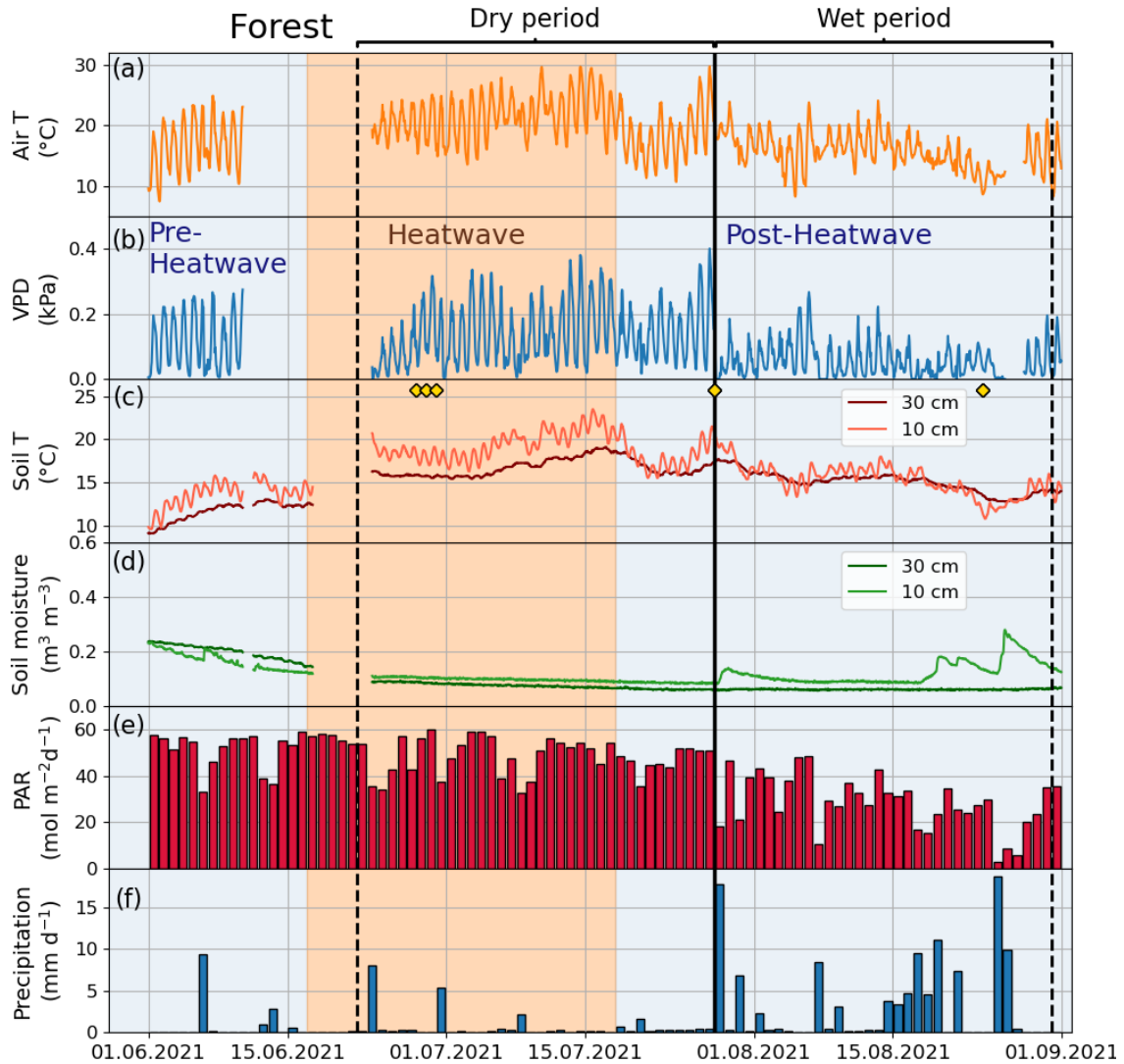


Figure A3. Meteorological condition at the Forest site showing hourly a) air temperature (Air T), b) water vapor deficit (VPD), c) soil temperature (Soil T) and d) soil moisture measured and e) daily mean photosynthetically active radiation (PAR) and daily sum precipitation data measured at the SMEARIII station. The yellow markers in panel (c) denote the dates of manual leaf gas measurements.

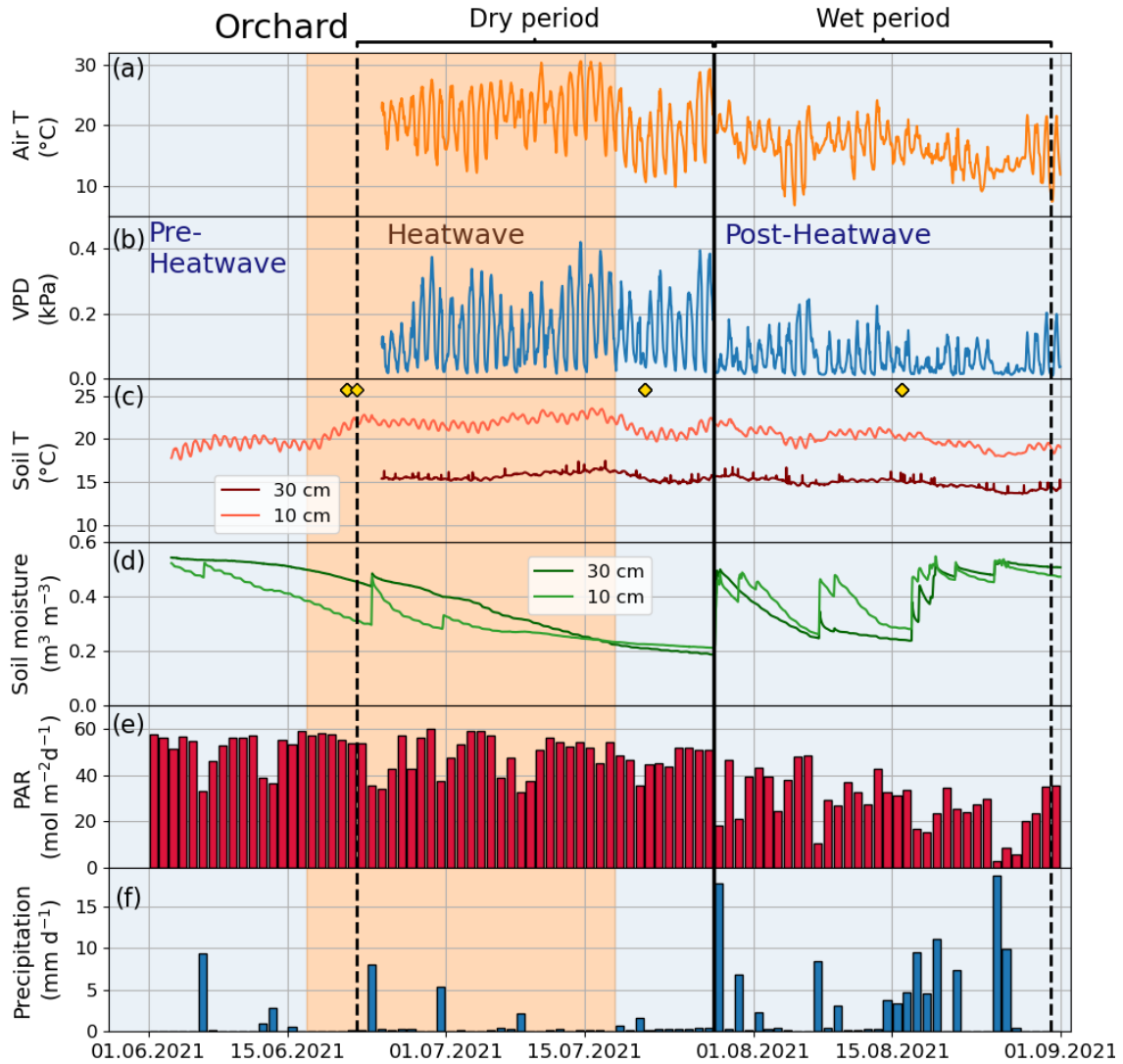


Figure A4. Meteorological condition at the Orchard site showing hourly a) air temperature (Air T), b) water vapor deficit (VPD), c) soil temperature (Soil T) and d) soil moisture measured and e) daily mean photosynthetically active radiation (PAR) and daily sum precipitation data measured at the SMEARIII station. The yellow markers in panel (c) denote the dates of manual leaf gas measurements.

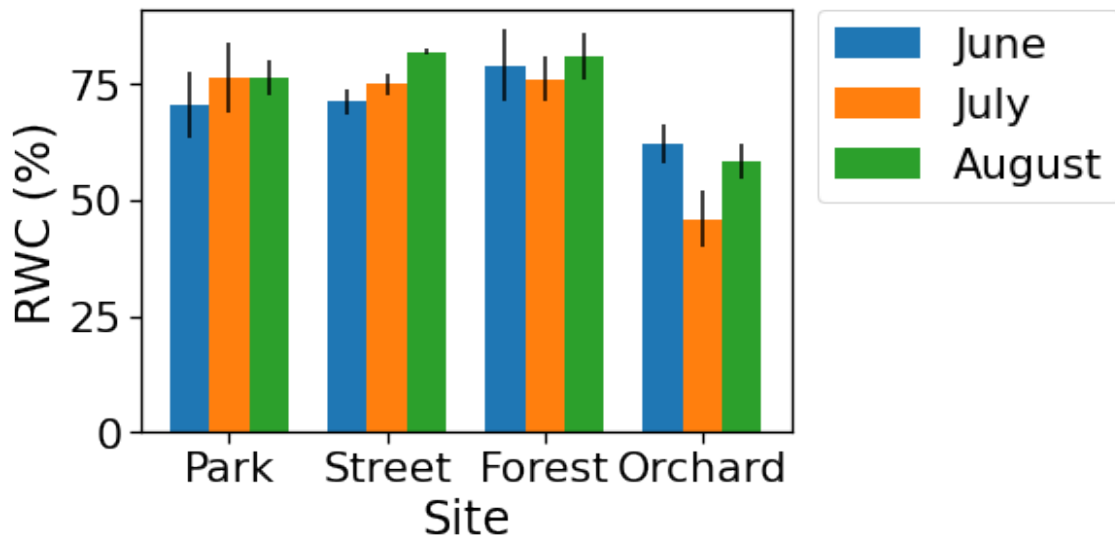


Figure A5. Monthly values of relative water content (RWC %) at the four urban sites.

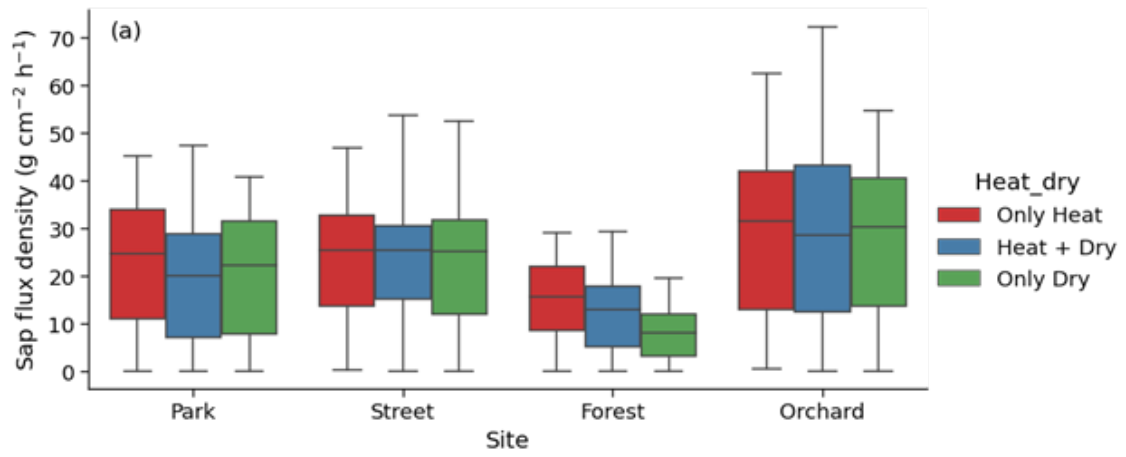


Figure A6. Pattern of sap flux density during heat and dry period at the four urban sites.

Author contributions. Conceptualization: JA, LK, LJ; Data collection: JA, JS, YF, AK, EK, EV; Formal analysis: JA, JS, AK; Funding acquisition: LK, LJ; Supervision: LK, LJ; Visualization: JA, JS; Writing–original draft preparation: JA; Writing–review and editing: JA, LK, LJ, YS, AL, EK. All authors have read and agreed to the article.

435 *Competing interests.* The authors declare that there is no conflict of interest.

Acknowledgements. We thank the Research Council of Finland (CarboCity projet, decision numbers: 321527 and 32554), the Research Council of Finland ACCC Flagship (decision numbers: 337549, 337552) and the Strategic Research Council working under the Research Council of Finland (CO-CARBON project, decision numbers: 335201 and 335204). This project has also received funding from the European Union’s Horizon 2020 research and innovation programme under grant agreement 101037319 (PAUL project). We would like to thank Erkki

440 Siivola, Jarkko Mäntylä, Elisa Vainio, and Teemu Paljakka for their technical support during the field measurements.

References

- Ahongshangbam, J., Kulmala, L., and Järvi, L.: Datasets of sap flow, meteorological, leaf gas measurements in urban green areas in Helsinki, <https://doi.org/10.5281/zenodo.7525319>, 2023.
- Atkin, O. K. and Tjoelker, M. G.: Thermal acclimation and the dynamic response of plant respiration to temperature, *Trends in Plant Science*, 8, 343–351, [https://doi.org/10.1016/S1360-1385\(03\)00136-5](https://doi.org/10.1016/S1360-1385(03)00136-5), 2003.
- 445
- Bowler, D. E., Buyung-Ali, L., Knight, T. M., and Pullin, A. S.: Urban greening to cool towns and cities: A systematic review of the empirical evidence, *Landscape and Urban Planning*, 97, 147–155, <https://doi.org/10.1016/j.landurbplan.2010.05.006>, 2010.
- Brack, C. L.: Pollution mitigation and carbon sequestration by an urban forest, *Environmental Pollution*, 116, S195–S200, [https://doi.org/10.1016/S0269-7491\(01\)00251-2](https://doi.org/10.1016/S0269-7491(01)00251-2), 2002.
- 450
- Bush, S. E., Pataki, D. E., Hultine, K. R., West, A. G., Sperry, J. S., and Ehleringer, J. R.: Wood anatomy constrains stomatal responses to atmospheric vapor pressure deficit in irrigated, urban trees, *Oecologia*, 156, 13–20, <https://doi.org/10.1007/s00442-008-0966-5>, 2008.
- Bussotti, F., Pollastrini, M., Killi, D., Ferrini, F., and Fini, A.: Ecophysiology of urban trees in a perspective of climate change., *Agrochimica*, 58, 247–268, <https://www.cabdirect.org/cabdirect/abstract/20153144491>, publisher: Università degli Studi di Pisa, 2014.
- Davies, Z. G., Edmondson, J. L., Heinemeyer, A., Leake, J. R., and Gaston, K. J.: Mapping an urban ecosystem service: quantifying above-ground carbon storage at a city-wide scale, *Journal of Applied Ecology*, 48, 1125–1134, <https://doi.org/10.1111/j.1365-2664.2011.02021.x>, [eprint: https://onlinelibrary.wiley.com/doi/pdf/10.1111/j.1365-2664.2011.02021.x](https://onlinelibrary.wiley.com/doi/pdf/10.1111/j.1365-2664.2011.02021.x), 2011.
- 455
- De Kauwe, M. G., Medlyn, B. E., Pitman, A. J., Drake, J. E., Ukkola, A., Griebel, A., Pendall, E., Prober, S., and Roderick, M.: Examining the evidence for decoupling between photosynthesis and transpiration during heat extremes, *Biogeosciences*, 16, 903–916, <https://doi.org/10.5194/bg-16-903-2019>, publisher: Copernicus GmbH, 2019.
- 460
- De Micco, V. and Aronne, G.: Morpho-Anatomical Traits for Plant Adaptation to Drought, in: *Plant Responses to Drought Stress: From Morphological to Molecular Features*, edited by Aroca, R., pp. 37–61, Springer, Berlin, Heidelberg, https://doi.org/10.1007/978-3-642-32653-0_2, 2012.
- Dhakar, S.: GHG emissions from urbanization and opportunities for urban carbon mitigation, *Current Opinion in Environmental Sustainability*, 2, 277–283, <https://doi.org/10.1016/j.cosust.2010.05.007>, 2010.
- 465
- Drake, J., Tjoelker, M., Varhammar, A., Medlyn, B., Reich, P., Leigh, A., Pfautsch, S., Blackman, C., López, R., Aspinwall, M., Crous, K., Duursma, R., Kumarathunge, D., De Kauwe, M., Jiang, M., Nicotra, A., Tissue, D., Choat, B., Atkin, O., and Barton, C.: Trees Tolerate an Extreme Heatwave via Sustained Transpirational Cooling and Increased Leaf Thermal Tolerance, *Global Change Biology*, 24, <https://doi.org/10.1111/gcb.14037>, 2018.
- Duarte, A. G., Katata, G., Hoshika, Y., Hossain, M., Kreuzwieser, J., Arneth, A., and Ruehr, N. K.: Immediate and potential long-term effects of consecutive heat waves on the photosynthetic performance and water balance in Douglas-fir, *Journal of Plant Physiology*, 205, 57–66, <https://doi.org/10.1016/j.jplph.2016.08.012>, 2016.
- 470
- Fischer, E. M. and Schär, C.: Consistent geographical patterns of changes in high-impact European heatwaves, *Nature Geoscience*, 3, 398–403, <https://doi.org/10.1038/ngeo866>, number: 6 Publisher: Nature Publishing Group, 2010.
- FMI: The Finnish Meteorological Institute, <https://en.ilmatieteenlaitos.fi/open-data>, 2021.
- 475
- Gebauer, T., Horna, V., and Leuschner, C.: Variability in radial sap flux density patterns and sapwood area among seven co-occurring temperate broad-leaved tree species, *Tree Physiology*, 28, 1821–1830, <https://doi.org/10.1093/treephys/28.12.1821>, 2008.

- Ghannoum, O. and Way, D. A.: On the role of ecological adaptation and geographic distribution in the response of trees to climate change, *Tree Physiology*, 31, 1273–1276, <https://doi.org/10.1093/treephys/tpr115>, 2011.
- 480 Gillner, S., Vogt, J., Tharang, A., Dettmann, S., and Roloff, A.: Role of street trees in mitigating effects of heat and drought at highly sealed urban sites, *Landscape and Urban Planning*, 143, 33–42, <https://doi.org/10.1016/j.landurbplan.2015.06.005>, 2015.
- Gillner, S., Korn, S., Hofmann, M., and Roloff, A.: Contrasting strategies for tree species to cope with heat and dry conditions at urban sites, *Urban Ecosystems*, 20, <https://doi.org/10.1007/s11252-016-0636-z>, 2017.
- Granier, A.: Une nouvelle méthode pour la mesure du flux de sève brute dans le tronc des arbres, *Annales des Sciences Forestières*, 42, 193–200, <https://doi.org/10.1051/forest:19850204>, publisher: EDP Sciences, 1985.
- 485 Granier, A., Bréda, N., Biron, P., and Villette, S.: A lumped water balance model to evaluate duration and intensity of drought constraints in forest stands, *Ecological Modelling*, 116, 269–283, [https://doi.org/10.1016/S0304-3800\(98\)00205-1](https://doi.org/10.1016/S0304-3800(98)00205-1), 1999.
- Hagemann, S. and Stacke, T.: Impact of the soil hydrology scheme on simulated soil moisture memory, *Climate Dynamics*, 44, 1731–1750, <https://doi.org/10.1007/s00382-014-2221-6>, 2015.
- Hardiman, B. S., Wang, J. A., Hutyra, L. R., Gately, C. K., Getson, J. M., and Friedl, M. A.: Accounting for urban biogenic fluxes in regional carbon budgets, *Science of The Total Environment*, 592, 366–372, <https://doi.org/10.1016/j.scitotenv.2017.03.028>, 2017.
- 490 Hartmann, H., Bastos, A., Das, A. J., Esquivel-Muelbert, A., Hammond, W. M., Martínez-Vilalta, J., McDowell, N. G., Powers, J. S., Pugh, T. A., Ruthrof, K. X., and Allen, C. D.: Climate Change Risks to Global Forest Health: Emergence of Unexpected Events of Elevated Tree Mortality Worldwide, *Annual Review of Plant Biology*, 73, 673–702, <https://doi.org/10.1146/annurev-arplant-102820-012804>, [_eprint: https://doi.org/10.1146/annurev-arplant-102820-012804](https://doi.org/10.1146/annurev-arplant-102820-012804), 2022.
- 495 Havu, M., Kulmala, L., Kolari, P., Vesala, T., Riikonen, A., and Järvi, L.: Carbon sequestration potential of street tree plantings in Helsinki, *Biogeosciences*, 19, 2121–2143, <https://doi.org/10.5194/bg-19-2121-2022>, publisher: Copernicus GmbH, 2022.
- Hernandez-Santana, V., Hernandez-Hernandez, A., Vadeboncoeur, M. A., and Asbjornsen, H.: Scaling from single-point sap velocity measurements to stand transpiration in a multispecies deciduous forest: uncertainty sources, stand structure effect, and future scenarios, *Canadian Journal of Forest Research*, 45, 1489–1497, <https://doi.org/10.1139/cjfr-2015-0009>, publisher: NRC Research Press, 2015.
- 500 Ibsen, P. C., Borowy, D., Dell, T., Greydanus, H., Gupta, N., Hondula, D. M., Meixner, T., Santelmann, M. V., Shiflett, S. A., Sukop, M. C., Swan, C. M., Talal, M. L., Valencia, M., Wright, M. K., and Jenerette, G. D.: Greater aridity increases the magnitude of urban nighttime vegetation-derived air cooling, *Environmental Research Letters*, 16, 034011, <https://doi.org/10.1088/1748-9326/abd8a>, publisher: IOP Publishing, 2021.
- Jim, C. Y. and Chen, W. Y.: Ecosystem services and valuation of urban forests in China, *Cities*, 26, 187–194, <https://doi.org/10.1016/j.cities.2009.03.003>, 2009.
- 505 Jo, H.-k.: Impacts of urban greenspace on offsetting carbon emissions for middle Korea, *Journal of Environmental Management*, 64, 115–126, <https://doi.org/10.1006/jema.2001.0491>, 2002.
- Järvi, L., Hannuniemi, H., Hussein, T., Junninen, H., Aalto, P. P., Hillamo, R., Mäkelä, T., Keronen, P., Siivola, E., Vesala, T., and Kulmala, M.: The urban measurement station SMEAR III: Continuous monitoring of air pollution and surface–atmosphere interactions in Helsinki, Finland, <https://helda.helsinki.fi/handle/10138/233627>, accepted: 2018-03-20T15:08:03Z Publisher: Boreal Environment Research Publishing Board, 2009.
- 510 Kjelgren, R. and Clark, J.: Microclimates and tree growth in three urban spaces, *Journal of Environmental Horticulture*, 10, 139–145, https://digitalcommons.usu.edu/psc_facpub/658, 1992.

- Konarska, J., Uddling, J., Holmer, B., Lutz, M., Lindberg, F., Pleijel, H., and Thorsson, S.: Transpiration of urban trees and its cooling effect
515 in a high latitude city, *International Journal of Biometeorology*, 60, 159–172, <https://doi.org/10.1007/s00484-015-1014-x>, 2016.
- Kunert, N. and Tomaskova, I.: Leaf turgor loss point at full hydration for 41 native and introduced tree and shrub species from Central
Europe, *Journal of Plant Ecology*, 13, 754–756, <https://doi.org/10.1093/jpe/rtaa059>, 2020.
- Kunert, N., Hajek, P., Hietz, P., Morris, H., Rosner, S., and Tholen, D.: Summer temperatures reach the thermal toler-
ance threshold of photosynthetic decline in temperate conifers, *Plant Biology*, n/a, <https://doi.org/10.1111/plb.13349>,
520 <https://onlinelibrary.wiley.com/doi/pdf/10.1111/plb.13349>, 2022.
- Lauri, P., Gorza, O., Cochard, H., Martinez, S., Celton, J.-M., Ripetti, V., Lartaud, M., Bry, X., Trottier, C., and Costes, E.: Genetic determin-
ism of anatomical and hydraulic traits within an apple progeny, *Plant, Cell & Environment*, 34, 1276–1290, <https://doi.org/10.1111/j.1365-3040.2011.02328.x>, 2011.
- Leuschner, C., Wedde, P., and Lübbe, T.: The relation between pressure–volume curve traits and stomatal regulation of water potential in five
525 temperate broadleaf tree species, *Annals of Forest Science*, 76, 1–14, <https://doi.org/10.1007/s13595-019-0838-7>, number: 2 Publisher: BioMed Central, 2019.
- Leuzinger, S., Vogt, R., and Körner, C.: Tree surface temperature in an urban environment, *Agricultural and Forest Meteorology*, 150, 56–62,
<https://doi.org/10.1016/j.agrformet.2009.08.006>, 2010.
- Lindén, J., Fonti, P., and Esper, J.: Temporal variations in microclimate cooling induced by urban trees in Mainz, Germany, *Urban Forestry
& Urban Greening*, 20, 198–209, <https://doi.org/10.1016/j.ufug.2016.09.001>, 2016.
530
- Liu, M., Pietzarka, U., Meyer, M., Kniesel, B., and Roloff, A.: Annual shoot length of temperate broadleaf species responses to drought,
Urban Forestry & Urban Greening, 73, 127–152, <https://doi.org/10.1016/j.ufug.2022.127592>, 2022.
- Lloyd, J. and Farquhar, G. D.: Effects of rising temperatures and [CO₂] on the physiology of tropical forest trees, *Philosophical Transactions
of the Royal Society B: Biological Sciences*, 363, 1811–1817, <https://doi.org/10.1098/rstb.2007.0032>, 2008.
- 535 Lu, P., Urban, L., and Zhao, P.: Granier’s thermal dissipation probe (TDP) method for measuring sap flow in trees: theory and practice,
<https://publications.csiro.au/rpr/pub?list=BRO&pid=procite:ac6fc6af-67dc-4b32-ac82-5d3c9678573a>, 2004.
- Marchin, R. M., Backes, D., Ossola, A., Leishman, M. R., Tjoelker, M. G., and Ellsworth, D. S.: Extreme heat increases stomatal conductance
and drought-induced mortality risk in vulnerable plant species, *Global change biology*, 28, 1133–1146, publisher: Wiley Online Library,
2022.
- 540 McCarthy, H. R. and Pataki, D. E.: Drivers of variability in water use of native and non-native urban trees in the greater Los Angeles area,
Urban Ecosystems, 13, 393–414, <https://doi.org/10.1007/s11252-010-0127-6>, 2010.
- Moser, A., Rahman, M. A., Pretzsch, H., Pauleit, S., and Rötzer, T.: Inter- and intraannual growth patterns of urban small-leaved lime (*Tilia
cordata* mill.) at two public squares with contrasting microclimatic conditions, *International Journal of Biometeorology*, 61, 1095–1107,
<https://doi.org/10.1007/s00484-016-1290-0>, 2017.
- 545 Muñoz-Vallés, S., Cambrollé, J., Figueroa-Luque, E., Luque, T., Niell, F. X., and Figueroa, M. E.: An approach to the evaluation and
management of natural carbon sinks: From plant species to urban green systems, *Urban Forestry & Urban Greening*, 12, 450–453,
<https://doi.org/10.1016/j.ufug.2013.06.007>, 2013.
- Nielsen, C., Bühler, O., and Kristoffersen, P.: Soil Water Dynamics and Growth of Street and Park Trees, *Arboriculture & Urban Forestry*,
33, 231–245, <https://doi.org/10.48044/jauf.2007.027>, 2007.
- 550 Nowak, D. J. and Crane, D. E.: Carbon storage and sequestration by urban trees in the USA, *Environmental Pollution*, 116, 381–389,
[https://doi.org/10.1016/S0269-7491\(01\)00214-7](https://doi.org/10.1016/S0269-7491(01)00214-7), 2002.

- Nowak, D. J., Greenfield, E. J., Hoehn, R. E., and Lapoint, E.: Carbon storage and sequestration by trees in urban and community areas of the United States, *Environmental Pollution*, 178, 229–236, <https://doi.org/10.1016/j.envpol.2013.03.019>, 2013.
- 555 Oke, T. R., Crowther, J. M., McNaughton, K. G., Monteith, J. L., Gardiner, B., Jarvis, P. G., Monteith, J. L., Shuttleworth, W. J., and Unsworth, M. H.: The micrometeorology of the urban forest, *Philosophical Transactions of the Royal Society of London. B, Biological Sciences*, 324, 335–349, <https://doi.org/10.1098/rstb.1989.0051>, publisher: Royal Society, 1989.
- Osone, Y., Kawarasaki, S., Ishida, A., Kikuchi, S., Shimizu, A., Yazaki, K., Aikawa, S.-I., Yamaguchi, M., Izuta, T., and Matsumoto, G. I.: Responses of gas-exchange rates and water relations to annual fluctuations of weather in three species of urban street trees, *Tree Physiology*, 34, 1056–1068, <https://doi.org/10.1093/treephys/tpu086>, 2014.
- 560 Paloheimo, E. and Salmi, O.: Evaluating the carbon emissions of the low carbon city: A novel approach for consumer based allocation, *Cities*, 30, 233–239, <https://doi.org/10.1016/j.cities.2012.04.003>, 2013.
- Pataki, D. E., Emmi, P. C., Forster, C. B., Mills, J. I., Pardyjak, E. R., Peterson, T. R., Thompson, J. D., and Dudley-Murphy, E.: An integrated approach to improving fossil fuel emissions scenarios with urban ecosystem studies, *Ecological Complexity*, 6, 1–14, <https://doi.org/10.1016/j.ecocom.2008.09.003>, 2009.
- 565 Pataki, D. E., McCarthy, H. R., Litvak, E., and Pincetl, S.: Transpiration of urban forests in the Los Angeles metropolitan area, *Ecological Applications*, 21, 661–677, <https://doi.org/10.1890/09-1717.1>, [_eprint: https://onlinelibrary.wiley.com/doi/pdf/10.1890/09-1717.1](https://onlinelibrary.wiley.com/doi/pdf/10.1890/09-1717.1), 2011.
- Pataki, D. E., Alberti, M., Cadenasso, M. L., Felson, A. J., McDonnell, M. J., Pincetl, S., Pouyat, R. V., Setälä, H., and Whitlow, T. H.: The Benefits and Limits of Urban Tree Planting for Environmental and Human Health, *Frontiers in Ecology and Evolution*, 9, <https://www.frontiersin.org/article/10.3389/fevo.2021.603757>, 2021.
- 570 Perini, K. and Magliocco, A.: Effects of vegetation, urban density, building height, and atmospheric conditions on local temperatures and thermal comfort, *Urban Forestry & Urban Greening*, 13, 495–506, <https://doi.org/10.1016/j.ufug.2014.03.003>, 2014.
- Rahman, M. A., Moser, A., Rötzer, T., and Pauleit, S.: Comparing the transpirational and shading effects of two contrasting urban tree species, *Urban Ecosystems*, 22, 683–697, <https://doi.org/10.1007/s11252-019-00853-x>, 2019.
- Rennenberg, H., Loreto, F., Polle, A., Brilli, F., Fares, S., Beniwal, R. S., and Gessler, A.: Physiological responses of forest trees to heat and 575 drought, *Plant Biology (Stuttgart, Germany)*, 8, 556–571, <https://doi.org/10.1055/s-2006-924084>, 2006.
- Riikonen, A., Järvi, L., and Nikinmaa, E.: Environmental and crown related factors affecting street tree transpiration in Helsinki, Finland, *Urban Ecosystems*, 19, 1693–1715, <https://doi.org/10.1007/s11252-016-0561-1>, 2016.
- Roth, M., Oke, T. R., and Emery, W. J.: Satellite-derived urban heat islands from three coastal cities and the utilization of such data in urban climatology, *International Journal of Remote Sensing*, 10, 1699–1720, <https://doi.org/10.1080/01431168908904002>, publisher: Taylor & 580 Francis [_eprint: https://doi.org/10.1080/01431168908904002](https://doi.org/10.1080/01431168908904002), 1989.
- RStudio Team: RStudio Integrated Development Environment for R, RStudio, PBC., Boston, MA, <httpwww.rstudio.com>, 2020.
- Rötzer, T., Moser-Reischl, A., Rahman, M. A., Hartmann, C., Paeth, H., Pauleit, S., and Pretzsch, H.: Urban tree growth and ecosystem services under extreme drought, *Agricultural and Forest Meteorology*, 308–309, 108 532, <https://doi.org/10.1016/j.agrformet.2021.108532>, 2021.
- 585 Schwaab, J., Meier, R., Mussetti, G., Seneviratne, S., Bürgi, C., and Davin, E. L.: The role of urban trees in reducing land surface temperatures in European cities, *Nature Communications*, 12, 6763, <https://doi.org/10.1038/s41467-021-26768-w>, number: 1 Publisher: Nature Publishing Group, 2021.
- Sjöman, H., Östberg, J., and Bühler, O.: Diversity and distribution of the urban tree population in ten major Nordic cities, *Urban Forestry & Urban Greening*, 11, 31–39, <https://doi.org/10.1016/j.ufug.2011.09.004>, 2012.

- 590 StromJan: StromJan/Raster4H: Final version, <https://doi.org/10.5281/zenodo.4005833>, 2020.
- Sushko, S., Yaroslavtsev, A., Tsuvareva, N., and Valentini, R.: Capacity of *Quercus robur* L. and *Tilia cordata* Mill. trees in providing urban ecosystem services in boreal climate, pp. EGU21–7125, <https://doi.org/10.5194/egusphere-egu21-7125>, conference Name: EGU General Assembly Conference Abstracts ADS Bibcode: 2021EGUGA..23.7125S, 2021.
- Urban, J., Ingwers, M. W., McGuire, M. A., and Teskey, R. O.: Increase in leaf temperature opens stomata and decouples net photosynthesis from stomatal conductance in *Pinus taeda* and *Populus deltoides* x *nigra*, *Journal of Experimental Botany*, 68, 1757–1767, <https://doi.org/10.1093/jxb/erx052>, 2017.
- 595 Vesala, T., Järvi, L., Launiainen, S., Sogachev, A., Rannik, , Mammarella, I., Ivola, E. S., Keronen, P., Rinne, J., Riikonen, A., and Nikinmaa, E.: Surface–atmosphere interactions over complex urban terrain in Helsinki, Finland, *Tellus B: Chemical and Physical Meteorology*, 60, 188–199, <https://doi.org/10.1111/j.1600-0889.2007.00312.x>, 2008.
- 600 Vicente-Serrano, S. M., Beguería, S., and López-Moreno, J. I.: A Multiscalar Drought Index Sensitive to Global Warming: The Standardized Precipitation Evapotranspiration Index, *Journal of Climate*, 23, 1696–1718, <https://doi.org/10.1175/2009JCLI2909.1>, publisher: American Meteorological Society Section: *Journal of Climate*, 2010.
- Villar-Salvador, P., Planelles, R., Oliet, J., Peñuelas-Rubira, J. L., Jacobs, D. F., and González, M.: Drought tolerance and transplanting performance of holm oak (*Quercus ilex*) seedlings after drought hardening in the nursery, *Tree Physiology*, 24, 1147–1155, <https://doi.org/10.1093/treephys/24.10.1147>, 2004.
- 605 Winbourne, J. B., Jones, T. S., Garvey, S. M., Harrison, J. L., Wang, L., Li, D., Templer, P. H., and Hutyrá, L. R.: Tree Transpiration and Urban Temperatures: Current Understanding, Implications, and Future Research Directions, *BioScience*, 70, 576–588, <https://doi.org/10.1093/biosci/biaa055>, 2020.
- Zapater, M., Bréda, N., Bonal, D., Pardonnet, S., and Granier, A.: Differential response to soil drought among co-occurring broad-leaved tree species growing in a 15- to 25-year-old mixed stand, *Annals of Forest Science*, 70, 31–39, <https://doi.org/10.1007/s13595-012-0233-0>, number: 1 Publisher: BioMed Central, 2013.